DIFFERENTIAL EXPRESSION OF APOPTOTIC GENES IN LUNG (A549) CANCER CELLS ESTABLISHED BY TREATMENT WITH *SENNA ITALICA* EXTRACTS

by

Moloantoa MI

[redacted]

Research Dissertation

Submitted in fulfilment of the requirements of the degree of

MASTER OF SCIENCE

in

BIOCHEMISTRY

in the

FACULTY OF SCIENCE AND AGRICULTURE

(School of Molecular and Life Sciences)

at the

UNIVERSITY OF LIMPOPO

(Turfloop Campus)

Supervisor: Prof LJ Mampuru

Co-Supervisors: Prof MP Mokgotho

: Dr KW Poopedi

2021

DECLARATION

I, Moloantoa Malose Ivan, declare that the dissertation hereby submitted to the University of Limpopo for the degree of Master of Science in Biochemistry has not been previously submitted by me for the degree at this or any other university, and that it is my own work in design and execution, and that all materials contained herein have been duly acknowledged.

Signature: _____

Date :__10 MARCH 2021____

DEDICATION

I would like to dedicate this work to the almighty God, my grandfather Moloantoa Malose J and My grandmother Moloantoa Mokgaetji E and my siblings Moloantoa Mokgaetji O, Moloantoa Ntsie L and my parents for all the support and love they have given me.

ACKNOWLEDGEMENTS

I would like to give thanks to the people and institutions listed below for their contributions and the success of this work:

1. Prof LJ Mampuru, Prof MP Mokgotho and Dr. KW Poopedi for their technical guidance and supervisory role in this project.

2. Ms MM Tolo, Ms MO Raboshakga, and all the academic staff members and cleaners in the BMBT department for their willingness to always help me.

3. University of Limpopo and SAMRC for the opportunity and financial support.

Glory be to GOD in the highest, the inventor of Biochemistry "Exodus 30 v 22-25".

Table of Contents

List of Figures

Chapter 2

Chapter 4

List of Tables

Abbreviations

A549	Adenocarcinoma human alveolar basal epithelial cells
AO	Acridine orange
BSA	Bovine serum albumin
cDNA	Complementary DNA
CEF	Chloroform: Ethyl acetate: Formic acid
CO_2	Carbon dioxide
Cyt c	Cytochrome c
DMEM	Dulbecco's modified eagle's medium
DMSO	Dimethyl sulfoxide
DNA	Deoxyribonucleic acid
DPPH	2,2-diphenyl-1-picrylhydrazyl
DSBs	DNA double strand breaks
EB	Ethidium bromide
EMW	Ethyl acetate : Methanol : Water
Fas-L	Fas ligand
FBS	Foetal bovine serum
H_2SO_4	Sulphuric acid
HEK 293	Human embryonic kidney 293 cells
IC_{50}	50% cytotoxic concentration
MTT	3-(4, 5-dimethylthiasol-2-yl)-2, 5-diphenyltetrasolium bromide
Na_2CO_3	Sodium carbonate
NaOH	Sodium hydroxide
NSCLC	Non-small cell lung cancer
PBS	Phosphate buffer saline
PCR	Polymerase chain reaction
PC3	Prostate cancer
PSN	Penicillin-Streptomycin-Neomycin
ROS	Reactive oxygen species
RPMI	Roswell Park Memorial Institute
SA	South Africa
Smac	Second Mitochondria-Derived Activator of Caspases
SCLC	Small cell lung cancer

SI	*Senna italica*
SIL	*Senna italica* leaf
SIR	*Senna italica* root
TEA	Toluene: Ethyl acetate: ammonia
TCA	Trichloroacetic acid
UV	Ultra violet radiation
WHO	World health organisation
ºC	Degrees Celsius
XIAP	X-linked inhibitor of apoptosis protein

ABSTRACT

Lung cancer is the most diagnosed cancer with an estimated 3 million deaths expected by 2035. Bioactive phytochemicals present in plants are preferred as anticancer therapeutic agents, due to their ability to differentiate between cancerous and normal cells. One such plant, *Senna italica,* is traditionally used to treat diabetes, malaria, constipation, jaundice, fever and sexually transmitted diseases. Several studies have reported on its anti-proliferative potential against different types of cancers. However, there is scanty information regarding its molecular mechanism of action against different types of cancers, more especially lung cancer. This study, therefore, aims to determine the differential expression profiles of apoptotic genes in lung A549 cancer cells induced by treatment with *S. italica* leaf and root extracts in an attempt to understand its purported anticancer molecular mechanism of action.

The leaves and roots of *S. italica* were dried in the dark and extracted with ethyl acetate and methanol. Screening for the presence of secondary metabolites was performed using thin layer chromatography and various standard chemical-based tests. The total phenolic and flavonoid compounds were evaluated using gallic acid and quercetin equivalence assays. The antioxidant activity of *S. italica* extracts was determined using DPPH free radical scavenging and ferric ion reducing power assays. The cytotoxicity of both leaf and root extracts on lung A549 cancer cells was evaluated using 3-(4,5-dimethylthiazol-2-yl)-2-5-diphenyl tetrazolium bromide (MTT) and further confirmed by Muse cell count and cell viability assays. The proliferation of cells, after treatment with different concentrations of the extracts, was examined using the Ki67 proliferation assay. Genotoxicity was determined to assess the potential damage caused by the extracts on the DNA using a MUSE^{TM} multicolour DNA damage kit following manufacturer's protocol. The morphological change of cells treated with different concentrations of *S. italica* ethyl acetate root extract was analysed using acridine orange/ ethidium bromide (AO/EB) dual staining assay and examined under fluorescent light. The total number of cells undergoing apoptosis was also determined using the Annexin V assay. The expression of 84 key genes, involved in programmed cell death or apoptosis, was determined using the Human Apoptosis RT^2 Profiler PCR array kit.

Senna italica methanol extract had a high content of plant materials in both leaves and roots compared to the ethyl acetate extract. A higher phenolic content was observed

mainly in the leaf extract and a higher flavonoid content was observed in the root extract. Phytochemicals, such as phenols, tannins, flavonoids, terpenoids and steroids, which are known to exhibit anti-cancer activity against cancerous cells were abundant in the ethyl acetate leaf and root extracts as compared to the methanol leaf and root extracts. Additionally, the ethyl acetate root extract exhibited more antioxidants and radical scavenging activity in comparison to the methanol root extract. The IC_{50} of ethyl acetate root extract was determined to be 200µg/ml. Both methanol and ethyl acetate root extracts had little to no effect on the viability of lung A549 lung cancer cells. The results were confirmed by cell count and viability assay results. The cytotoxicity of ethyl acetate root extract was also evaluated against the normal kidney HEK-293 cells, which displayed little cytotoxic effect. The proliferation results indicated that *S. italica* ethyl acetate root extract has the potential to reduce the proliferation of lung A549 cancer cells. The ethyl acetate root extract was found to induce late apoptosis in A549 cells, but the genotoxicity data indicated that the DNA double strand breaks (DSBs) were repairable. The results further showed an expression of different genes that inhibit apoptosis, such as XIAP in lung A549 cells, following treatment with *S. italica* ethyl acetate root extract. In conclusion, the ethyl acetate root extract displayed a promising anti-cancer therapeutic potential, and thus warrants further investigation to elucidate the identity of the inherent chemical components that are responsible for the observed biological activity.

CHAPTER 1: INTRODUCTION

The lung cancer epidemic was first noted in the 1940s in the United States of America (USA) and other European countries among males (Franceschi and Bidoli, 1999). The early studies around the 1950s demonstrated that cigarette smoking was the cause of lung cancer, supported by epidemiological and toxicological evidence (Franceschi and Bidoli, 1999). The lung cancer cases are estimated to be 247 270 (116 980 females and 30 340 male cases) in 2020 (Alexander *et al*., 2020). Lung cancer in Africa ranks fourth compared to all other cancers that affect men, with about 39 300 new estimated cases per year with a mortality rate of 37 700 people. The highest incidence of lung cancer is in the North of Africa (Shankar *et al*., 2019). In sub-Saharan Africa, there are high smoking related diseases with the prevalent lung cancer subtype in South Africa being adenocarcinoma (Koegelenberg *et al*., 2016). In South Africa, between the years 1995 to 2006, there was a decrease in mortality among men with an increase in women (Shankar *et al*., 2019).

New technologies used to classify lung cancer have given a clearer understanding of the disease. One of the critical steps in lung cancer is understanding the pathogenesis and tumour biology (Zheng, 2016). The histology of the lung is used to classify two groups of lung cancers; the small cell (SCLC) and non-small cell (NSCLC) lung cancer. The most prevalent type of lung cancer is non-small cell lung cancer (NSCLC) which is further classified as squamous cell, large cell and adenocarcinoma cancers (Bradley *et al*., 2019). Small-cell lung cancer (SCLC) is a metastatic type of lung cancer that is lethal and highly aggressive with an estimated 250 000 deaths each year worldwide, and a reported minimal survival rate of 7% in five years (Gazdar *et al*., 2017). The characteristics of SCLC include early metastatic dissemination, genomic instability and tumour growth. Most of the patients suffering from SCLC are former or current heavy smokers (Gazdar *et al*., 2017).

The NSCLC causes about 85% of the total lung cancers. The prevalent type is the adenocarcinoma subtype which causes 40% of lung cancers, while the squamous cell carcinoma subtype, caused by cigarette smoking, accounts for 25% to 30% and large cell carcinoma only 5-10% (Zappa and Mousa, 2016). The non-small cell lung cancer adenocarcinoma subtype has been reported to affect both women and men and is not age specific. All people are vulnerable to lung cancer because radon chemicals in the environment and passive smoking can lead to the development of the disease.

Lung cancer is treated using different methods depending on the type of lung cancer and the stage of the disease. The small cell lung cancer, which causes a small percentage of total lung cancers, is treated using chemotherapy, radiotherapy and surgery. The treatment of non-small cell lung cancer is managed through the understanding of the patient's disease stage, cell type histology and molecular profile (Kalemkerian, 2016). Adenocarcinoma is the prevalent type of all lung cancers but, despite the extensive research on adenocarcinoma treatment, there is still a decline in the effectiveness of treatment because of its resistance to chemotherapies and radiotherapies (Denisenko *et al*., 2018). The challenge with lung cancer treatment, as compared to other cancers, is that the disease is rarely detected at an early stage. Failure of early diagnosis leads to the ineffectiveness of chemotherapy in patients at a late stage with little chance of survival (Brainard and Farver, 2019).

The development of cancer treatment at an advanced stage, using cytotoxic combination chemotherapy influenced by age, histology and comorbidity, is the first line of cure. Cisplatin is regarded as a more effective platinum-based treatment, however it is associated with some additional side effects (Zappa and Mousa, 2016).

Despite the development in research efforts, extensive drug discovery and developments made towards the therapeutic strategies, there are still challenges linked to lung cancer treatment that result in a high mortality rate in metastatic patients. Regardless of the development made in improving the 5-year survival of lung cancer, it is still regarded as one of the worst among all cancers at 17,7% over the past 50 years. Due to all these challenges, the development of anticancer therapy that is effective and lacks side effects is currently desirable (Singh *et al*., 2016).

Traditional medicines are described by the World Health Organisation as the skills, practices and knowledge that belong to a particular culture based on their beliefs, theories and experiences used for prevention, diagnosis and to maintain healthy human beings (Ly, 2018). Medicinal plants are rich in antioxidants and contribute to the discovery of novel drugs with anticancer properties and fewer side effects. There is a need for investigations of plants that show promising activity against cancer because only a small portion of the plant population has been studied (Priya *et al.*, 2015). *Senna italica* is one of the herbs used in traditional medicine and it contains constituents with different biological activities, such as antimicrobial, antiallergic, antiparasitic, anti-inflammatory, antioxidant, antitumour, and anti-proliferative

properties (Maia *et al*., 2019; Masoko *et al*., 2010). Methanol and ethyl acetate extracts of *S. italica* have shown a reduction in proliferation of prostate cancer cells (PC3), breast cancer cells (MCF-7) and hepatocellular carcinoma cells (HePG-2) *(Khalaf et al*., 2019). However, there is limited information on the molecular mechanism of action used by the plant against different cancers. This study, therefore, aims to elucidate the molecular mechanisms of apoptosis induced by extracts of *S. italica* on lung A549 cancer cells.

CHAPTER 2: LITERATURE REVIEW

2.1 Development and classification of lung cancer stages

Lung cancer is a highly heterogeneous disease as it can develop from many various sites represented by signs and symptoms based on its anatomic location. Additionally, about 70% of patients with lung cancer are characterised at stage III or stage IV, already in the advanced stage (Lemjabbar-Alaoui *et al*., 2015). The disease is further anatomically classified as depicted in Figure 2.1, based on the primary tumour extent, the regional lymph nodes involvement and the absence or presence of distant metastatic spread, at stage I and stage II the tumour is still small and at stage III tumour invades other part of the body including diaphragm and chest wall and stage IV there is a development of distant metastasis. Moreover, normal cells can convert into malignant lung cancer following different steps involving epigenetic and genetic changes (Lemjabbar-Alaoui *et al*., 2015).

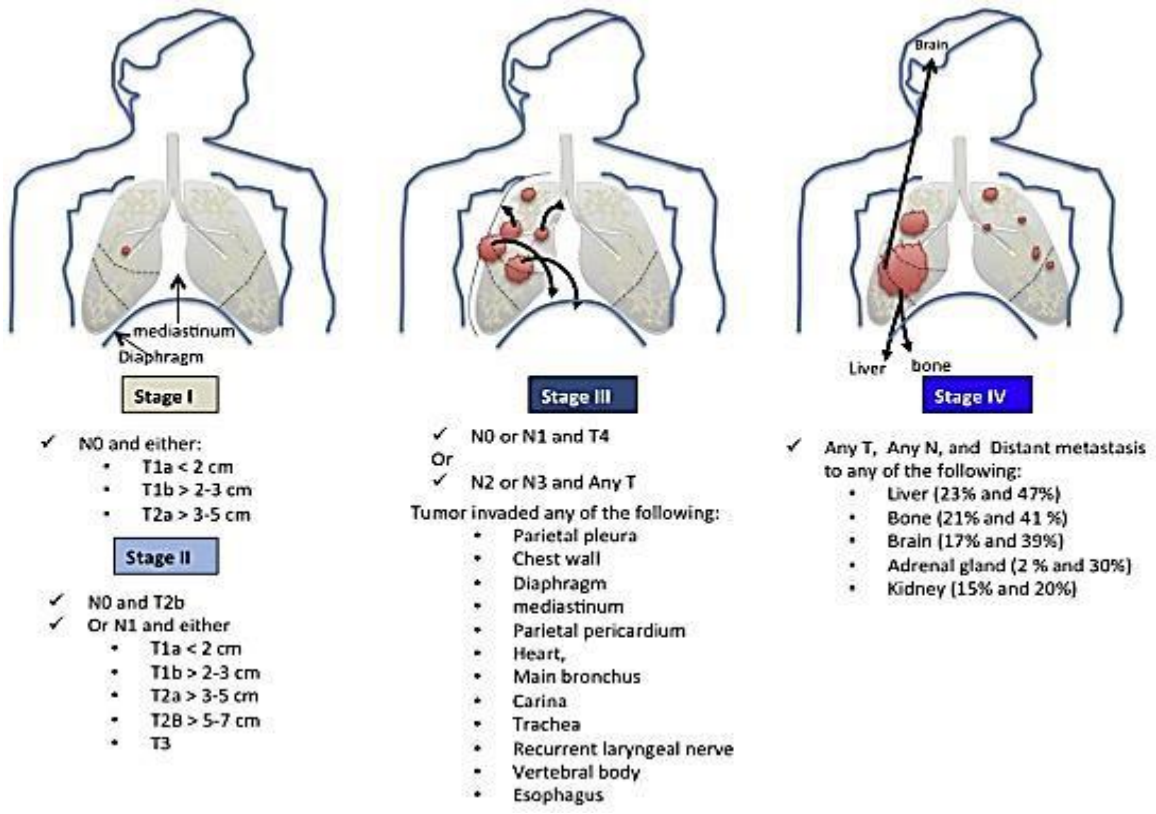

Figure 2.1: The non-small cell lung cancer staging schematic representation. The four stages (stage I, II, III and IV) of non-small lung progression showing the invasion of tumour at stage III and stage IV showing high percentage of distant metastasis at organs such as Liver. T = size and extent of the primary tumour, N = extent of involvement of regional lymph nodes and M= presence and absence of distant metastatic spread.

2.2 1 Smoking and lung cancer risk

Several studies have shown that over 90% of lung cancer deaths are caused by smoking, while other cancers develop from different inhaled carcinogens after a long-term exposure (Gomes *et al*., 2017). Smoking has been reported to be the main contributor in the development of lung cancer. About 73 carcinogens, e.g. polonium radioactive isotope and NNK,1,3-butadiene, from cigarette smoke are known (Mustafa *et al*., 2016b). In more than 70% of men and 55% of women with death caused by lung cancer, the major cause is tobacco smoking (O'Keeffe *et al.,* 2018). There are still challenges in lung cancer investigation in order to fully outline and understand the specific mechanisms (Figure 2.2) in which smoking initiation or nicotine addiction causes carcinogens followed by the DNA adducts which lead to mutation in KRAS, TP53, and other genes leading to lung cancer due to low apoptosis, and understanding can contribute to new insights, as well as general cancer prevention (Hecht, 2012). Despite smoking being known as the predominant cause of lung cancer, there is an increased risk of 16-19% of lung cancer developing from second hand smoke from the environment, and those living with people who smoke having 20-30% risk of developing lung cancer (Mustafa *et al*., 2016a).

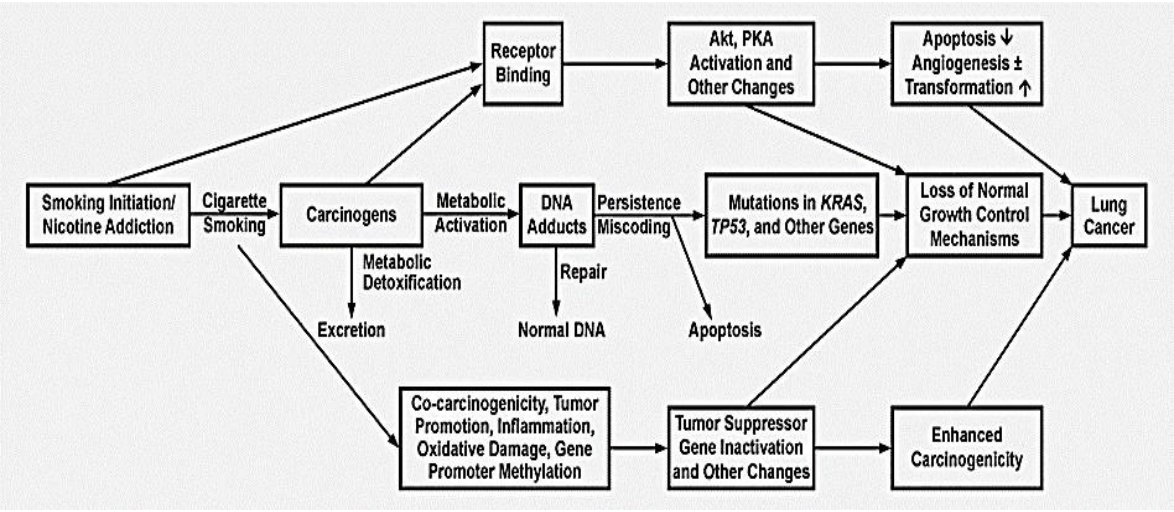

Figure 2.2: The presentation of how lung cancer is caused by smoking cigarette. The diagram and arrows further show the events that drive the formation of lung cancer from smoking. (Figure adapted from Hecht, 2012).

2.2.2 Second-hand smoke exposure

Cigarette smoking is a prevalent cause of lung cancer, however occupational and environmental exposure are also considered as factors that contribute to lung cancer (Kurt *et al*., 2016). Studies have revealed the detection of 4-(methylnitrosamino)-1-(3-pyridyl)-1-butanone (NNK), which is known to be the cause of adenocarcinoma in smokers and in the urine of non-smokers. This is evidence that indicates second hand smoke is responsible for lung cancer (Kim *et al*., 2018). The indoor air pollution that results from second hand smoke, intrusion of the ambient air pollution, volatile organic compounds, and solid fuels combustion from cooking and home heating can also be a source of exposure (Kurt *et al*., 2016). Amongst all other air pollutants, vehicle emissions account for 25 to 40% of total air pollution. Nitrogen monoxide released by vehicles is oxidised to nitrogen dioxide which is involved in different phytochemical reactions induced by sunlight (Chen *et al*., 2015). Studies have shown that the DNA lesions in the lung can develop into different diseases, mutations and cancers due to sulphur dioxide inhalation (Chen *et al*., 2015). The lung injury caused by microorganisms and air pollutant inhalation leads to formation of reactive nitrogen species and reactive oxygen species (Gomes *et al*., 2017).

2.3 Reactive oxidative species (ROS)

The reactive oxygen species (ROS) are free radicals responsible for oxidative stress in the cells leading to an inflammatory response (Shaikh *et al*., 2016). The small molecules derived from oxygen include oxygen radicals such as peroxyl (RO_2), hydroxyl (OH^-), alkoxyl (RO) and superoxide (O_2^-), and others that can be easily converted into radicals e.g., ozone (O_3), hypochlorous acid (HOCl), hydrogen peroxide (H_2O_2) and singlet oxygen (O_2) or their oxidizing agents (Prasad *et al*., 2017). The reactive oxygen species in the body are involved in the pathogenesis of different human diseases, though they are beneficial at low concentrations, regulating homeostasis and intracellular signalling. However at high concentrations the lipids, DNA and protein are damaged, resulting in various diseases (Figure 2.3) (Prasad *et al*., 2017). The cellular environment rich in inflammatory cells leads to higher potential of cell proliferation that results in the upregulation of growth factors. Inactivation of apoptosis & cytokines and DNA damage is caused by high production of reactive oxygen species and reactive nitrogen species. Inflammation ensures steady physiological functions by removing pathogenic and injured tissues (Gomes *et al*.,

2017).

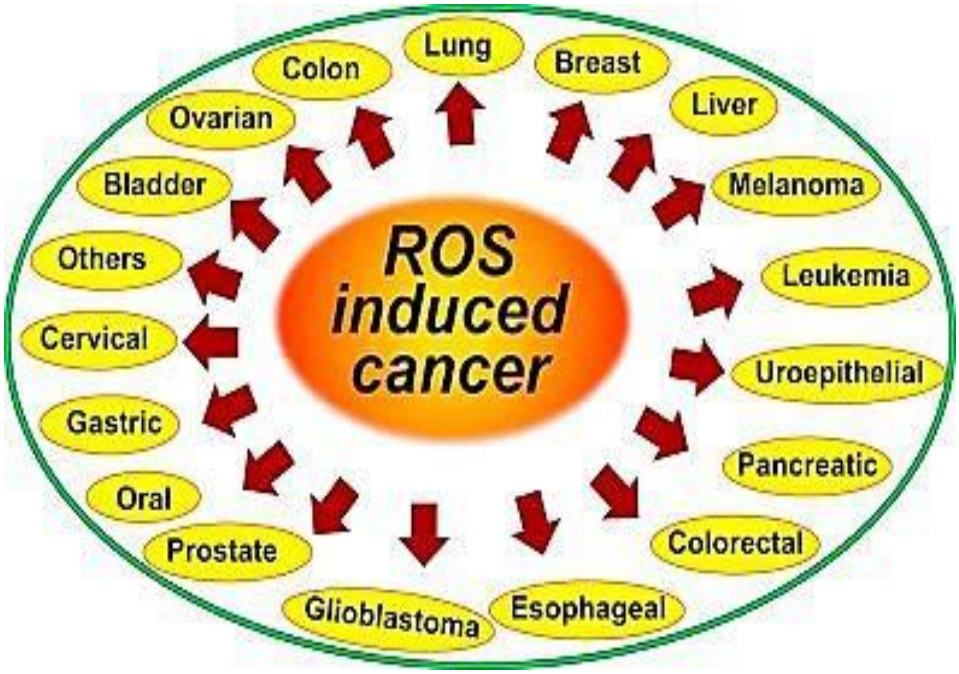

Figure 2.3: Overproduction of reactive oxygen species causes multiple cancers. The ROS induced cancer leads to lung cancer (Prasad *et al*., 2017).

2.4 Tumour microenvironment

The tumour microenvironment is a heterogeneous environment of different types and subtypes of cells that cause cancer manifestations and accommodate the tumour to ensure the continuous evolution of cancer and causing more deaths (Shishir *et al*., 2018). Uncontrollable growth of cells (Figure 2.4), with no functional purpose, is known as a tumour and they can spread to other cells or organs in the body and cause cancer. However not all tumours have the potential to cause cancer. Benign tumours remain at their primary site of origin and are not cancerous (Wang *et al*., 2018). Tumour microenvironment components encourage cancer cell proliferation while avoiding apoptosis and hypoxia inhibition, as well as impeding the immune system, supporting the invasion and distant organ metastasis through activation of the immune cells (Shishir *et al*., 2018).

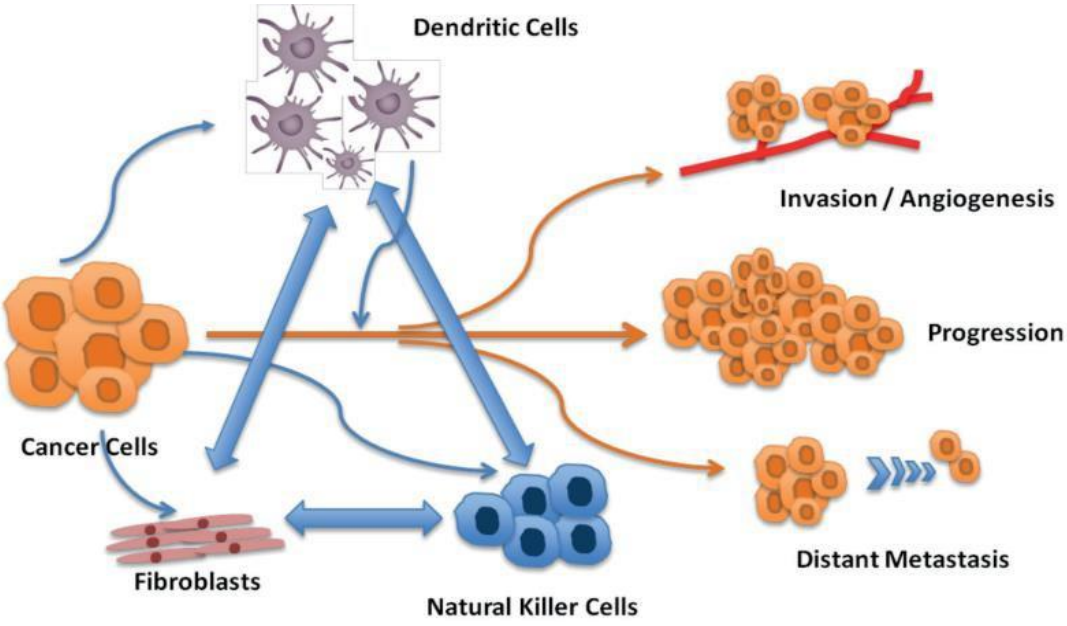

Figure 2.4: The tumour microenvironment that contributes to the formation of metastasis, progression and invasion (Wang *et al*., 2018). The resultant cancer cells can subsequently undergo invasion, progression or distant metastasis.

2.5 Metastasis

Metastasis is a process in which cancer cells move from their site of primary tumour origin to spread and settle at other different sites. About 90 % of cancer deaths are caused by metastasis and not the primary tumour (Guan, 2015). Metastasis of lung cancer can result in different undesirable effects such as weight loss, muscular atrophy, malaise, and depletion of fat reserves, general weakness and cancer cachexia (Milovanovic *et al*., 2017).

2.6 The new era of drugs development for cancer treatment and the challenges

Despite this exciting era of new drug development, some challenges hinder the synthesis of drugs, including cost and trial failure. This is caused by complex diseases that cannot be cured using a single target due to the nature of the disease and the different pathogenic pathways of tissue and organ, interconnecting at different levels to form a disease (Li and Weng, 2017). Radiotherapy uses an x-ray of high energy and destroys the localised tumours. However it has side effects such as a sore throat, cough, fatigue and skin burn in the region of tumour. The disadvantage of chemotherapy is their circulation in the entire body, as a result the healthy tissues are damaged while trying to treat cancer cells (Sudhakar, 2009). The limitations and challenges with the current drugs are their effects on normal cells and as a result, the

undesired side effects, including neurotoxicity, cardiotoxicity and hair loss. Cancer cells may become resistant to drugs due to mutation, and the development of a drug that will be selective to only cancerous cells is the driving force of research (Singh *et al*., 2016). There are new drugs developed for lung cancer treatment, such as the platinum based drugs, but they are coupled with various side effects (Dilruba and Kalayda, 2016).

2.6.1 Platinum-based cancer therapy

The platinum-based drugs support clinical drugs used for the treatment of solid tumours including colorectal, genitourinary and the non-small lung cancers. Cisplatin has been used for over three decades as the prominent anticancer drug (Wang and Guo, 2013). Cisplatin has been used as a single therapeutic modality, or in combination with different cytotoxic agents and radiotherapy (Wang and Guo, 2013). However platinum- based anticancer drugs are associated with different side effects, such as poor specificity, as well as systematic disorders, such as ototoxicity, nephrotoxicity and neurotoxicity, and, during treatment, emetogenesis imposes serious disorders or injuries on patients (Wang and Guo, 2013).

2.7 Apoptosis

Intracellular and extracellular signals activate the apoptotic pathway, a process that is highly regulated to remove unwanted and unnecessary cells activated by various conditions (Claire M Pfeffer and Singh, 2018). The characteristics of apoptosis include DNA cleavage, morphological changes, nuclear fragmentation and chromatin condensation. It occurs in two major pathways, namely the intrinsic and extrinsic pathways, and both have the potential to cause caspase cascade activation. As a result, they trigger different steps of biochemical events that result in morphological changes leading to death (Syed Abdul Rahman *et al*., 2013). Although apoptosis is regarded as a well-defined process of cell death that occurs frequently, other types of cell death are non-apoptotic types and are also of biological importance (Leist and Jäättelä, 2001). The natural compounds that are found in medicinal plants are known to have the potential to target the tumour through the control of cell death via the apoptosis intrinsic and extrinsic pathways (Figure 2.5) (Aung *et al*., 2017).

2.7.1 Intrinsic pathway

The different endogenous and exogenous stimuli activate the intrinsic pathway, i.e. oxidative stress, ischemia and DNA damage, which plays a major role in the development and removal of the damaged cells. The Bcl-family members, Bcl-2 and Bax (anti-apoptotic and pro-apoptotic regulatory proteins), that are attached to the mitochondrial membrane influence the intrinsic pathway (Loreto *et al*., 2014). As a result of the pro-apoptotic signalling in the intrinsic pathway, there is a perturbation of the mitochondrial membrane and cytochrome C is released into the cytoplasm, leading to a complex formation or apoptosome through apoptotic protease activating factor 1 (APAF1) and caspase-9 in an inactive form. The cleavage and activation of caspase 9 occurs through adenosine triphosphate, hydrolysed by the complex, then the active form of caspase-9 follows by activation of different caspases (Caspases-3, -6 and -7) which leads to apoptosis (Loreto *et al*., 2014).

2.7.2 Extrinsic pathway

The extrinsic pathway is the process that induces apoptosis, triggered by an extracellular signal, and these death signals or death ligands bind to the tumour necrosis factor. There are different types of death ligands, such as tumour necrosis factor, tumour necrosis related apoptosis inducing ligand and Fas ligand (Fas-L) (Pfeffer *et al*., 2018). They recruit the adaptor protein to bind to the death receptor and, as a result, the death-inducing signalling complex (DISC) is formed, followed by initiator procaspase-9 and procaspase-10 binding. The procaspases are then activated by this death-inducing signal complex after binding, thus leading to cell death following the cleavage of proteins and cytoskeleton through activation of the executioner caspases-3, -6 and -7 (Pfeffer *et al*., 2018).

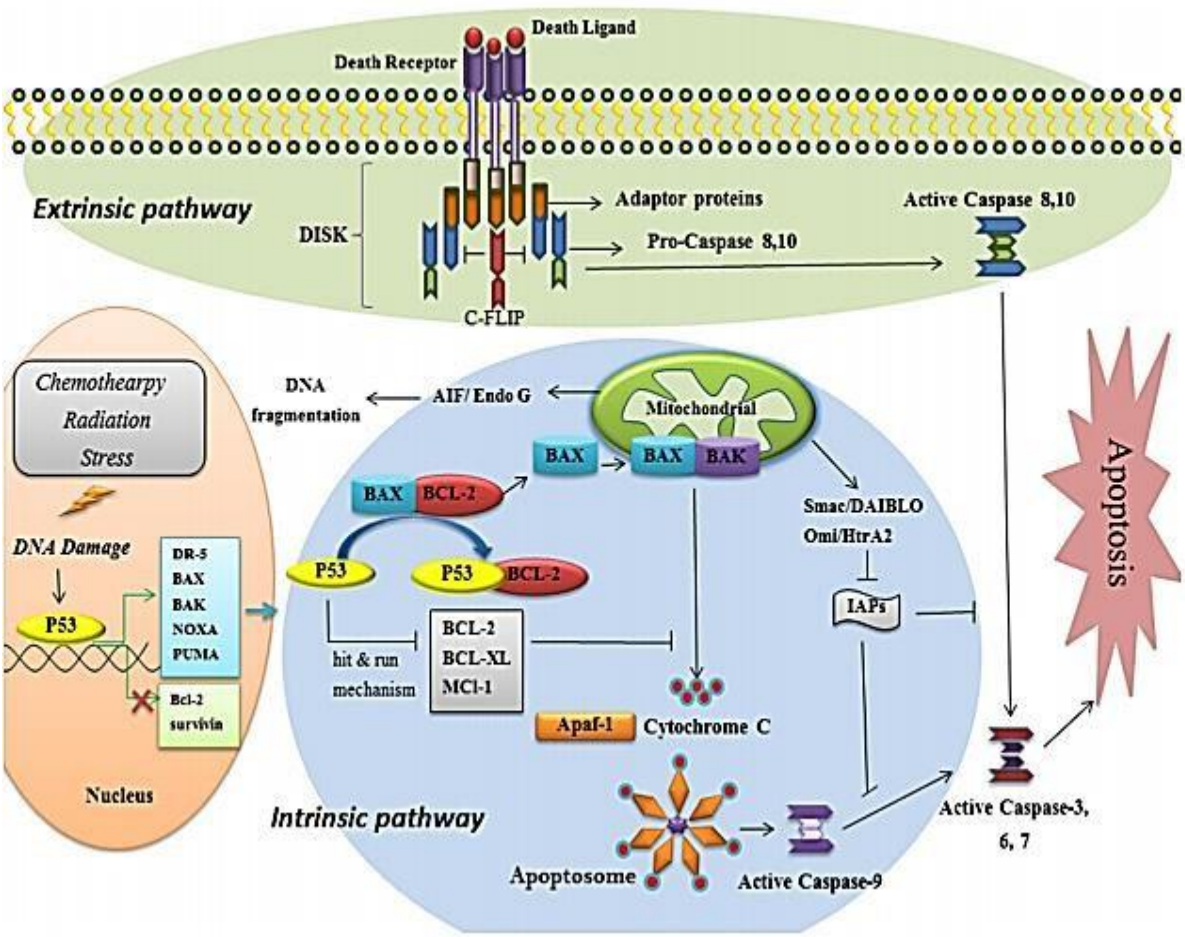

Figure 2.5: The intrinsic and extrinsic apoptotic pathways. The diagram shows radiation stress-induced DNA damaged after chemotherapy, followed by p53 activation leading to the release of cytochrome C from the mitochondria and subsequent activation of the mediator and executioner caspases culminating to an apoptotic cell death (Goldar *et al*., 2015).

2.8 Morphological features of apoptosis and necrosis

The morphological features of apoptosis are nuclear fragmentation, chromatin condensation in the nucleus and the roundup of the cells, followed by a decrease in cellular volume. Some of the morphological features of later stage apoptosis include cytoplasmic organelles ultrastructural modification, blebbing of membrane and membrane integrity loss (Wong, 2011). Necrosis has necrotic or necrosis morphological features (Figure 2.6) involving the organelles swelling, cell volume gain, rupture of plasma membrane followed by intracellular contents' loss. Various factors lead to necrotic cell death. Cellular and organelle processes, cause inflammation, triggered through the release of the intracellular damage associated molecular patterns (DAMPs) by the lytic nature of necrosis, leading to many diseases due to the disturbance between the balance of apoptosis and necrosis (Chaabane *et al*., 2013; Zhang *et al*., 2018)

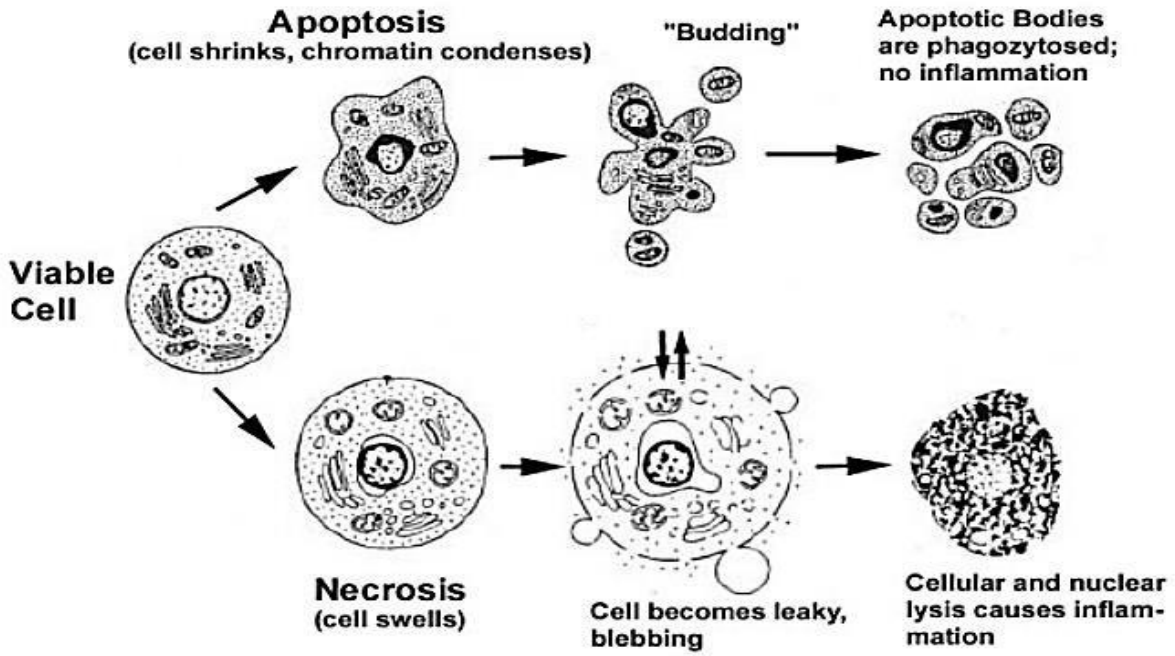

Figure 2.6: The Apoptosis and Necrosis cell death processes. The apoptotic pathway results in the generation of "still viable" apoptotic bodies that are phagocytosed by macrophages, resulting in a clean cell death process with no inflammation, while the necrotic cell death results in leaky cellular and nuclear lysis causing an inflammatory response (Gewies, 2003).

2.8.1 The signalling of apoptosis regulatory mechanisms

Apoptosis is activated when specific death inducing signals are encountered. Caspases are known to play an important role as the initiators and executioners of apoptosis. They are the cysteinyl-dependent aspartate directed protease family and control apoptosis at a cellular level and, as a result through the cascade of molecular events, cause cellular demise. They are activated through various commonly known pathways. The intrinsic pathway is activated when an internal injury affects the cell, caused by intrinsic stresses including hypoxia, oncogenes and direct DNA damage. The extrinsic pathway affects the outer cell, caused by a signal that dictates cell death. It may also occur via the less known pathways, such as the intrinsic endoplasmic reticulum pathway (Palai and Mishra, 2014: Wong, 2011).

2.8.1.1 p53 protein

p53 protein is a well-known tumour suppressor protein, also known as TP 53 or tumour protein 53, and it was so named because of its molecular weight size of 53 kDa. It is a cellular protein found in cancerous cell nuclei and tightly binds to the large T antigen simian virus 40 (SV40) (Chaabane *et al*., 2013). p53 plays various roles in genomic stability, angiogenesis, differentiation and6 apoptosis after DNA damage. p53 is induced and activated to block the late G1 phase, resulting in DNA repair. However in

human cancers some mutations inactivate p53 leading to impaired control of the cell cycle. Moreover, mutations can accumulate, leading to increased cancer risk and then the role of p53 is to transactivate different genes that function in DNA repair, cell-cycle and apoptosis (Maxwell and Davis, 2000).

2.8.1.2 Bcl-2 family

A gene family, B cell-lymphoma 2 (*bcl*-2), encodes over 20 proteins. The role of the protein is to ensure the balance between survival and death of cells. It was found to be part of the chromosomal translocation t(14;18) that occurs in follicular lymphoma patients, leading to an elevated transcription of Bcl-2 due to large B cell lymphoma diffusion (Ashkenazi *et al*., 2017). There are different family members of Bcl-2 which possess Bcl-2 homology domains (BH1, BH2, BH3 and BH4). The four domains of BH are present in Bcl-2 and Bcl-x and are known to play a role in apoptosis inhibition. The family members of Bcl-2 anti-apoptotic plays a role of inhibiting apoptosis through antagonizing the actions of family members of Bcl-2 pro-apoptotic (Bax, Bok and Bak) which have the domains BH1, BH2 and BH3. The BH3 short motif is possessed by the BH3 proteins including Hrk, Bad, Noxa, Bim, PUMA, Bid, Bmf, and Blk (Ashe and Berry, 2003).

2.8.1.3 Caspases

Cysteine aspartate specific proteases (caspases) are an intracellular protein family that are involved in the process of apoptosis. When the cells commits to die, they are at a stage called apoptotic commitment and this occurs due to the activation of execution caspases (Pfeffer and Singh, 2018). The caspases have a role in inflammation and apoptosis, however not all family members of caspases, their targets and physiological roles are well characterised. The caspases are produced as procaspases and at their aspartate residue, they are processed proteolytically to produce their active forms (Ashe and Berry, 2003).

2.9 Traditional medicine

Traditional medicine is described as mixtures that are complex with a variety of compounds i.e. infusions, extracts, essential oils and tinctures. Plants were used for over 600 years by humans as a source of traditional medicine due to their ability to treat different diseases (Yuan *et al*., 2016). Substances with defined chemical constituents are defined as drugs and different drugs that are currently used are synthesised from animals and plants. Plants, without any scientific proof, were used as drugs for many centuries with the knowledge being passed on from one generation to the next. However there are challenges regarding the use of traditional medicines according to WHO (1978). One of the challenges is that traditional medicines don't keep pace with modern technology, as well as scientific advancement, since the methods and training are often kept secret. Secondly, the use of traditional medicines is influenced by beliefs and traditions which are difficult to rationalise (Taylor *et al*., 2001). Since 1980s, the developed countries started to show interest in indigenous traditional knowledge, and it led to more research conducted to produce non-toxic inexpensive drugs from plants. The search of traditional medicine for different ailment cures has led to the discovery of novel drugs, which can be used for diverse disease treatment. According to the scientific reports, over 80% of the population in Africa and Asia depend on traditional medicine as their source for disease treatment and health needs (Oyebode *et al*., 2016).

2.9.1 The plant Senna italica

Senna italica is a small herb of the Fabaceae family (Figure 2.7) and has green leaves, pale green stems with yellow flowers and grows up to two feet in height (Dabai *et al*., 2012). Fabaceae belongs to the legumes with about 19 000 species and 730 genera, and about 350 species of this flowering plant. *Senna italica* is found mainly in the tropical and subtropical areas. Reports claim secondary metabolites of various chemical classes, such as anthraquinones and flavonoids. These secondary metabolites have been reported to have biological and pharmacological properties, including laxative, anti-ulcerogenic, antifungal, cytotoxic, anti-inflammatory, hepatoprotective and antioxidant capabilities (De Albuquerque Melo *et al*., 2014). The different species of plant were used by traditional healers for sexually transmitted and intestinal diseases, as well as for rheumatic, laxative, and purgative purposes. The different parts of *Senna italica* plant have been reported to have different biological

activities, such as cytotoxicity, antioxidant, antimicrobial and antiproliferative. *Senna italica* plant extract is found to have bioactive compounds which exhibit its anti-cancerous and anti-inflammatory activities (Jothi *et al*., 2015).

Figure 2.7: The picture of a flowering *Senna italica* plant. The plants' yellow flowers and green leaves are clearly visible. The picture was taken at Bolahlakgomo village, Zebediela in the Limpopo Province, South Africa.

2.10 Bioactive compounds

The bioactive compounds in plants can be described as secondary metabolites, produced within the plants, which are not needed for daily primary functioning and growth of the plant. The bioactive compounds in man and animal are known to have both pharmacological and toxicological effects. The intake of these compounds in the body is known to have a different outcome at a certain dosage; they are known to be either healthy, curative or can be deadly when consumed at a higher dosage (Bernhoft *et al*., 2008). The bioactive compounds give the plant activity to be effective against different diseases. The flavonoids are responsible for the protection of free radicals produced during photosynthesis and the terpenoids are known to have a function in attracting seed dispersers or pollinators. The new drugs discovery results from natural products derived from plant extract, as a standardized extract or as pure products.

Phytochemicals in plants are known to have less adverse effects. However clinical trials are still required for determination of safer use despite a claim from many people on the benefit from herbals (Duistermaat and Kolk, 2000).

2.10.1 Phenolics

Phenolics, produced from the plants in the Shikimic acid and the phenolic compounds, are the secondary metabolites. The phenolic compounds range from a simple to an extremely polymerized compound and they contain a benzene ring with one or more hydroxyl groups. Polyphenols contain different compounds, such as the simple flavonoids, complex flavonoids and the phenolic acids, and they are definite types of secondary metabolites distributed in all the metabolic processes in the plant. The phenolics have advantages such as anti-inflammatory, anti-aging, antiproliferative and antioxidant agents (Lin *et al*., 2016).

2.10.2 Terpenoids

Terpenoids are one of the largest groups of natural products, composed of a two five-carbon (isoprenoid units) as a building block, and they are classified into several groups such as monoterpenes, diterpenes and triterpenes depending on the building block. They are of plant origin, with the exception of some being synthesized as part of primary or secondary metabolites by organisms, such as the bacteria and yeast. Monoterpenes are known to prevent and also act as therapy for different cancers, such as the forestomach, pancreatic, skin, lung and prostate carcinomas (Thoppil and Bishayee, 2011).

2.10.3 Flavonoids

Flavonoids are a plant group of secondary metabolites with more than 9000 molecules readily available in the plant organs and tissues. They are found only in higher plants, pteridophytes and bryophytes, and play a major role in plants, due to their involvement in various processes such as pollination, plant-pathogen interactions and seed development, and their genes are induced following conditions such as wounding and metal toxicity (Hernández *et al*., 2009). The experimental discovery indicates the importance of flavonoids as anticarcinogenic and their effect in inflammation, invasion, metastasis and proliferation (Romagnolo and Selmin, 2012). The classification of

flavonoids (figure 2.8) is based on the oxidation degree of the ring shape of ring C and ring B connection position (T. yang Wang *et al*., 2018).

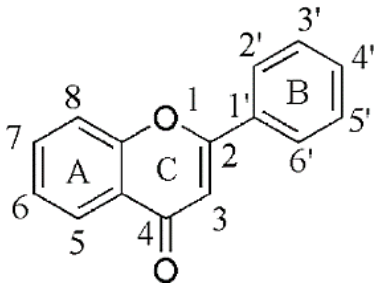

Figure 2. 8: The structure of basic flavonoids (Wang *et al*., 2018).

2.10.4 Tannins

Tannins are phenolic compounds with a higher molecular weight that ranges from 500 to over 3000 Daltons (Da) and they are located in plant tissue vacuoles in the wood, bark, fruit, leaves and roots. Their role has been linked to a plant protection mechanism against insects, birds and mammalian herbivores (Hassanpour *et al*., 2011). They are of interest due to their health importance in inflammatory and cardiovascular matters, and their potential effect as an antiviral, antitumour and antimicrobial, as well as their role in the essential immune response (Ropiak *et al*., 2016). There are two classes of tannins (figure 2.9), the hydrolysable polyhydric alcohol and the condensed tannins (non-hydrolysable) which have been reported to have a therapeutic effect with claims to be effective against cardiovascular disorders, allergies, treatment of tumours and to reduce cancer risk (Ghosh, 2015).

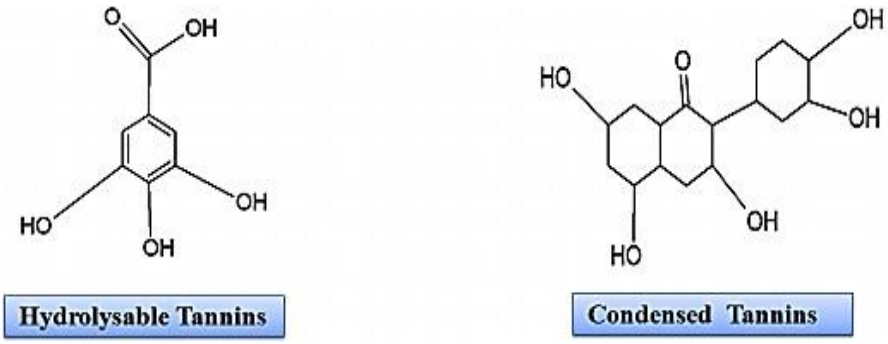

Figure 2. 9: The structure of hydrolysable and condensed tannin (Ghosh, 2015).

2.10.5 Steroids

Steroids are a cholesterol group formed from lipophilic compounds with a lower molecular weight. They are derived from or found in different terrestrial, synthetic and marine sources, and different classes of steroids have a biochemistry and physiology significant role in the living organism where they are found (Sultan, 2015). Steroids are reported to have anticancer properties and this is due to their potential to initiate apoptosis through inhibition of glycolysis, the NF-κB pathway and intracellular levels variation of K^+, H^+, Ca^{2+} and Na^+ (Sawadogo *et al*., 2012). The source of isolation, pharmacological activities and chemical structure are used to classify the steroids and the ones derived from the plants possess various health benefits, such as hepatoprotective and antitumor properties (Patel *et al*., 2015). The steroids are formed from cholesterol and they all have a common ringed structure (Figure 2.10) of perhydro-1,2-cyclopentenophenanthrene, and different types of steroids are formed by adding side chains (Sultan, 2015)

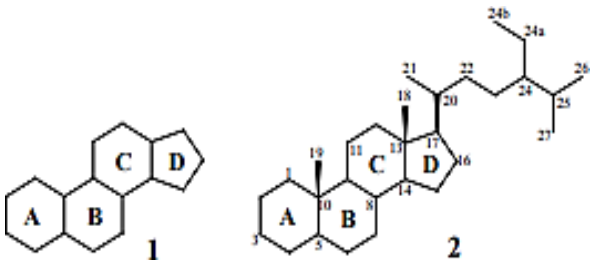

Figure 2.10: The common steroid ring 1, a perhydro-1,2-cyclopentenophenanthrene and 2, an example of a typical steroid with more side chains (Sultan, 2015).

2.11. Aim of the study

The study aimed to evaluate the cytotoxicity of the leaf and root extracts of *Senna italica* and their effects on the differential expression of apoptotic genes in lung A549 cancer cells.

The objectives of the study were to:

i. Analyse the phytochemical constituents of the *S. italica* leaves and roots extracts.
ii. Evaluate the effects of *S. italica* extracts on the viability and proliferation of lung A549 cancer cells and HEK 293 normal kidney cells using (3-(4, 5-dimethylthiazol-2-yl)-2, 5-diphenyltetrazolium bromide) (MTT) and the MUSE^{TM} Ki67 proliferation assays, respectively.
iii. Determine the mode of cell death triggered by the exposure of lung A549 cancer cells to extracts of *S. italica* using the annexin V assays.
iv. Assess the potential genotoxic effects of *S. italica* extracts using MUSE^{TM} multicolour DNA damage kit.
v. Determine the expression profiles of the various apoptotic genes of extract treated lung A549 cancer cells using a human apoptosis RT^2 profiler PCR Array kit.

CHAPTER 3: MATERIALS AND METHODS

3.1 Reagents and Equipment

Series 25 shaking incubator (New Brunswick Scientific Co Inc., U.S.A), sodium carbonate (Na_2CO_3), ethyl acetate and methanol, iron (III) chloride ($FeCl_3$) TLC (thin layer chromatography), acetone, toluene, ethyl acetate, ammonia, chloroform, ethyl acetate, formic acid, 2,2-diphenyl-1-picrylhydrazyl (DPPH), H_2SO_4 (sulphuric acid), Folin-Ciocalteu, sodium carbonate, aluminium chloride, potassium acetate, quercetin dimethyl sulfoxide (DMSO), 3-(4,5-dimethylthiazol-2-yl)-2-5-diphenyl tetrazolium bromide (MTT) (Sigma-Aldrich). Spectrophotometer, L-ascorbic acid, non- coated plates, microtiter-plate multimode detector (Promega-Glomax multi detection system). Lung A549 and Hek-293 kidney cells American Type Culture Collection (ATCC; Manassas, VA, USA). Roswell Park Memorial Institute (RPMI) 1640 Medium, Dulbecco's Minimum Eagles Medium (DMEM) (HyClone Laboratories, South Logan, USA). Foetal bovine serum (FBS) Penicillin-Streptomycin-Neomycin (PSN) and trypsin (Gibco, Life technologies, USA). Phosphate-buffered saline (PBS) (Lonza, Verviers, Belgium). Muse™ cell count and viability assay kit, Muse Ki67 proliferation assay, multicolour DNA damage kit, Muse™ cell analyser (Merck-Millipore, Germany).

3.2. Plant harvest and extraction

The *Senna italica* plant (UNIN 11129) was collected from Bolahlakgomo village, Zebediela in the Limpopo Province, South Africa, and authentication was confirmed by the Larry Leach Herbarium (UNIN) at the University of Limpopo. The leaves and roots were dried in the dark at room temperature, ground to powder, using a mechanical blender, and stored in airtight glass jars until use. Twenty grams of leaf and root material was weighed and extracted with 200 mL of each solvent [ethyl acetate and methanol in a ratio of 1:10 (w/v)] according to a published method (Eloff, 1998). The resultant extracts being termed SIL-EA (*S. italica* ethyl acetate leaf extract), SIL-Met (*S. italica* methanol leaf extract), SIR-EA (*S. italica* ethyl acetate root extract) and SIL-Met (*S. italica* methanol leaf extract). The extracts were incubated in a Series 25 shaking incubator set to 220 rpm at room temperature for 24 hrs. After filtration, the 3 hr interval was followed by 1 hr with filtration into pre-weighed glass vials and the filtrate dried under a stream of air until dry. The dried extracts were weighed again for total yield determination and further experiments.

3.3 Thin layer chromatography

The fingerprint analyses of SIL-EA, SIL-Met, SIR-EA and SIL-Met were determined on TLC plates coated with silica gel. A 10 mg/mL stock solution of all extracts were prepared by dissolving 10 mg of dried samples into 1 mL of acetone. 10 mL of each sample was loaded on a TLC plate divided into 50 x 100 in size. Different mobile phases were prepared for maximum separation of extract constituents by eluting TLC plates in mobile phases of varying polarities i.e. TEA (toluene: ethyl acetate: ammonia) non-polar, CEF (chloroform: ethyl acetate: formic acid) intermediate non-polar and EMW (ethyl acetate : methanol : water) polar. After elution of extract constituents, the solvent front was drawn at the top of the plate and allowed to dry under the fume hood before visualization under the UV-light, at different wavelengths (254 nm and 365 nm). The plates were sprayed with freshly prepared 0.2% of DPPH in methanol and vanillin/H_2SO_4 (0.1 g vanillin, 28 mL methanol, 1 mL sulphuric acid) and heated in an oven at 110°C for maximum colour development, according to the method of (Kotzé and Eloff, 2002).

3.4 Qualitative phytochemical analysis

The presence of terpenoids, tannins, flavonoids, steroids and phenols were determined according to different published methods.

3.4.1 Terpenoids

The presence of terpenoids was confirmed using the Salkowski test. Briefly, SIL-EA, SIL-Met, SIR-EA and SIL-Met were mixed with 3 ml of concentrated H_2SO_4 and 2 mL of chloroform. The positive results for the presence of terpenoids were indicated by the formation of a reddish-brown interface (Sheel *et al*., 2014).

3.4.2 Tannins and Phenols

The presence of tannins and phenols was confirmed by adding 2 mL of 2% iron (III) chloride ($FeCl_3$) and mixing with the crude extracts. The positive results for the presence of tannins and phenols were indicated by a blue-green or black colour (Vaghasiya *et al*., 2011).

3.4.3 Flavonoids

The flavonoids presence was confirmed by adding 3 mL of crude extracts and mixing with 1 mL of 10% of sodium hydroxide (NaOH). The positive results for the presence of flavonoids were indicated by yellow colouration development (Dabai *et al*., 2012).

3.4.4 Steroids

The presence of steroids was confirmed by adding 2 mL of chloroform and 2 mL of concentrated H_2SO_4. The positive results for the presence of steroids were indicated by a red colour formed in the lower chloroform layer (Vaghasiya *et al*., 2011).

3.5 Quantitative analysis

3.5.1 Phenolic content

The total phenolic content of SIL-EA, SIL-Met, SIR-EA and SIL-Met was determined by the Folin-Ciocalteu method with some modifications. The total phenolic content of ethyl acetate and methanol extracts was determined by mixing 100 µL of each extract (10 g/L) with 50 µL of Folin-Ciocalteu reagent. The mixture was incubated in the dark at room temperature and, after 5 minutes, the reaction was terminated by adding 500 µL 7% Na_2CO_3. The standard curve of gallic acid (0,0625 to 1 mg/mL) was prepared by mixing 100 µL of gallic acid with 50 µL of Folin-Ciocalteu reagent. The mixture was incubated in the dark at room temperature and, after 5 minutes, the reaction was terminated by adding 500 µL 7% Na_2CO_3. The mixture was allowed to stand for 90 minutes in the dark at room temperature and absorption was measured at 750 nm. The phenolic compound in ethyl acetate and methanol extracts was determined by the following formula: C = c.V/m (Akula and Odhay, 2013

Where: C = total phenolic content of compounds (mg/g) of plant extract n GAE; c = the gallic acid concentration established from the calibration curve (mg/ml); v= the extract volume in mL; and m = the weight of the pure plant ethyl acetate and methanol extracts in grams.

3.5.2 Flavonoid content

The total flavonoid content of the *S. italica* extracts was determined using the aluminium chloride colorimetric assay. A stock solution of all extracts at a concentration of 10 mg/mL was prepared. One hundred microliters of the plant extract

were mixed with 10% aluminium chloride (100 µL), 1 M potassium acetate (100 µL) and distilled water (2800 µL). The mixture was incubated for 30 minutes at room temperature. A set of reference standard solutions of quercetin (0,0625 to 1 mg/mL) was prepared similarly to the plant extract. The absorbance of test and standard solutions was measured at 510 nm using a spectrophotometer and the reactions were carried out in triplicates. The total flavonoid content was expressed as mg of quercetin equivalent (QE)/g determined by linear regression from a quercetin standard curve (Chang *et al*., 2002)

3.6 Antioxidant assays

The antioxidant activity of *S. italica* extracts was determined spectrophotometrically using DPPH free radical scavenging and ferric ion reducing power assays.

3.6.1 Quantitative DPPH free radical scavenging activity assay

The antioxidant activity of *S. italica* ethyl acetate and methanol extracts was determined quantitatively using DPPH free radical scavenging assay. Different concentrations (0 µg/ml to 1000 µg/ml) of SIL-EA, SIL-Met, SIR-EA, SIL-Met and the positive control L-ascorbic acid were prepared in non-coated plates. In each well, an equal volume of 0,2% (w/v) DPPH dissolved in methanol was added and the mixture was incubated for 30 minutes at room temperature. The absorbance of the decrease in the DPPH purple colour was measured at 490 nm using the microtiter-plate multimode detector.

$$\% \text{ inhibition} = \frac{Ac-As}{AC} \times 100$$

Where Ac is the absorbance of the control, and As is the absorbance of the sample

3.6.2 Ferric ion reducing power assays

The ferric ion reducing power of *S. italica* ethyl acetate and methanol extracts was determined using the method described by Benzie and Strain, (1996)**.** Different concentrations (0 µg/mL to 1000 µg/mL) of each extract were prepared in a non-coated well plate. The solutions were mixed with 250 µL 0.2M phosphate buffer (pH 7.4) and 250 µL potassium ferricyanide (1% w/v prepared in distilled water). The mixture was incubated for 20 minutes at 50°C. After incubation, 250 µL trichloroacetic acid (10%

w/v prepared in distilled water) was added to each well. The mixture was centrifuged at 3000 rpm for 10 minutes and the supernatant was transferred into a new non-coated well plate. The supernatant was mixed with 250 µL distilled water and 50 µL freshly prepared ferric chloride (0,1% w/v prepared in distilled water). L-ascorbic acid was used as positive control while the blank was prepared with an equal volume of water without adding an extract. The absorbance was measured at 700 nm wavelength using a multimode detector.

% reducing power = % inhibition = $\frac{(A700\,nm\,of\,sample-1)}{(A700\,nm\,of\,blank)}$) x 100

3.7 Cell maintenance

The cancerous lung A549 and normal HeK-293 kidney cell lines were purchased from American Type Culture Collection. Lung A549 and Hek-293 cells were maintained in RPMI 1640 Medium and DMEM, respectively, supplemented with 10% FBS and 1% PSN at 37°C in a humidified atmosphere at 95% air and 5% CO_2. Cells were allowed to grow to a confluence of 80% and sub-cultured or maintained frequently. Before experiments or sub-culturing, the cells were washed with 10% PBS and detached with 0.05% trypsin.

3.8 Cell viability and cytotoxicity assays

The viability of the lung A549 cancer and Hek-293 normal kidney cells was assessed using the MTT assay by a method previously reported by Cole (1986). The cells were plated at a density of 1 x 10^6 cells per mL in 96 well plates. The cells were treated with 100 µg/mL to 800 µg/mL of SIL-EA, SIL-Met, SIR-EA and SIL-Met and incubated for 24 hrs. The treatment media was removed and 20 µL MTT (1 mg/mL) was added to each well and incubated for 4 hours. The MTT solution was decanted and 50 µL DMSO was added to each well and incubated for 30 minutes, to dissolve the formazan product. The absorbance was measured using multimode detector at an absorbance of 560 nm. The percentage inhibition was calculated using this formula:

Viability percentage = $\frac{(A_{560nm}\text{ of sample})}{(A_{560nm}\text{ of control})}$ x 100

The results of the MTT assay were confirmed using the Muse™ cell count and viability assay kit according to the manufacturer's instructions. The cells were seeded at a density of 1 x 10^6 cells/mL, and treated with 100 µg/mL to 800 µg/ml SIR-EA. Following 24 hrs of treatment, the cells were washed twice with 100 µL of PBS and detached by the addition of trypsin. The mixture was centrifuged, the supernatant was removed, the pellet resuspended in 50 µL of media and mixed with 450 µL of count and viability reagent. After incubation at room temperature for 5 minutes, the results were analysed using the Muse™ cell analyser

3.9. Proliferation assay

The Muse Ki67 proliferation assay was performed according to the manufacturer's protocol. The lung A549 cancer cells were seeded in a 48 well plate and allowed to attach overnight at 1 x 10^6 per mL, followed by treatment with 100 µg/mL and 200 µg/mL SIR-EA. Curcumin (70 µM) served as a positive control and DMSO served as a negative control. After 24 hrs of treatment, cells were washed with 1 x PBS and detached using trypsin, and a concentration of 1.0 x 10^5 of cells was transferred into a new tube. A 50 µL of the fixation solution was added to each tube and incubated at room temperature. After incubation, 150 µL assay buffer was added, centrifuged and the supernatant removed. A 100 µL permeabilisation solution was added to each tube followed by incubation at room temperature for 15 minutes. After incubation, a 100 µL 1x assay buffer was added, centrifuged and the supernatant was removed. Fifty microliters (50 µL) 1 x assay buffer was added to each well, mixed and incubated for 15 minutes at room temperature. After incubation, 10 µL of Muse Hu IgG1-PE was added to one tube of untreated cells and Muse Hu Ki67-PE was added to the others. The solution was mixed and incubated at room temperature for 30 minutes. After the incubation, 150 µL 1 x assay buffer was added to each tube. The results were analysed by Muse™ cell analyser (Merck-Millipore, Germany).

3.10 Genotoxicity assay

MUSE™ multicolour DNA damage kit was performed to assess the potential damage caused by the extracts on the DNA. Lung A549 cancer cells, at a concentration of 2 x $10^{5,}$ were seeded in a 48 well plate and allowed to attach overnight. The cells were then treated with 100 µg/ml and 200 µg/ml SIR-EA for 24 hrs and 70 µM curcumin served as a positive control. After 24 hrs of treatment, the cells were detached,

transferred into tubes, centrifuged at 1330 rpm for 5 minutes and media was discarded. Following centrifugation, the cells were resuspended by adding 100 µL 1 x Assay Buffer per 200 000 cells and 100 µL Fixation Buffer was added at a ratio of 1:1 and the sample was mixed by pipetting thoroughly followed by 10 minutes incubation on ice. After incubation, the cells were centrifuged at 1330 rpm for 5 minutes and the supernatant was removed and 200 µL ice cold 1 x Permeabilisation Buffer was added and the cells were incubated on ice for 10 minutes. Following incubation, cells were centrifuged at 1 330 rpm for 5 minutes and the supernatant was discarded followed by resuspension one word of cells in 180 µL 1 x Assay Buffer. An antibody working cocktail solution (10 µL) was added to cells and incubated for 30 minutes at room temperature in the dark. Following incubation, 100 µL 1 x Assay Buffer was added to each sample and centrifuged for 5 minutes at 1330 rpm, and the supernatant was discarded. The cells were resuspended in 200 µL 1 x Assay Buffer and analysed using the Muse^{TM} cell analyser

3.11 Cell death analyses

3.11.1. Acridine orange and ethidium bromide dual staining assay

The A549 cells were seeded at a concentration of 1 x 10^5 in a 48 well plate and allowed to attach overnight. Following incubation, the cells were treated for 24 hrs with 100 and 200 µg/ml SIR-EA and 70 µM curcumin respectively. Following incubation, cells were washed twice with 300 µL 1 x PBS followed by staining with 100 µL 1 µg/mL acridine orange and ethidium bromide and incubated for 10 minutes in the dark. The cells were washed again twice with 300 µL 1 x PBS. The cells were viewed and photographed under the 10x objective using a fluorescence microscope

3.11.2 Annexin V & dead cell apoptosis assay

The lung A549 cancer cells were seeded at a concentration of 1 x 10^5 in a 48 wells plate and allowed to attach overnight. The cells were then treated with 100 µg/mL and 200 µg/mL SIR-EA and 70 µM curcumin for 24 hrs. Following treatment, 100 µL of cells were re-suspended in 1% FBS and 100 µL of Muse™ Annexin V & Dead Cell Reagent were added. The mixture was thoroughly mixed, followed by staining at room temperature for 20 minutes in the dark. The results were analysed after incubation using the Muse cell analyser

3.12 Human apoptosis RT^2 profiler PCR Array.

3.12.1 RNA extraction

The total RNA was isolated from the A549 cancer cells using the Qiagen RNAeasy mini kit according to the manufacture's protocol. The A549 cells were seeded in a flask at a concentration of 1 x 10^6 and treated with 200 µg/mL *S. italica* and 70 µM curcumin for 24 hrs in an incubator at 37°C. After 24 hrs of treatment, the cells were washed with 4 mL 1 x PBS and 2 mL trypsin was added to the flask to detach the cells. For lysis, a 350 µL buffer RLT (with 10 µL β-mercaptoethanol in 1 mL) was added to the cells. A 350 µL 70% ethanol was added to the lysate and 700 µL was transferred to an RNeasy mini spin column and centrifuged at speed of ≥ 800 x g for 15 s. A buffer RW1 (700 µL) was added to the precipitate, centrifuged at a speed of ≥ 800 x g for 15 s and the pellet was collected. The supernatant was discarded and 500 µL buffer RPE was added to the spin column and centrifuged at speed ≥ 3000 rpm. The same step was repeated twice and finally the RNA was eluted by centrifugation with RNase-free water (50 µL) at a speed of ≥ 3 000 rpm for 60 s.

3.12.2 DNase digestion

Buffer RW1 (350 µL) was added to an RNeasy column and centrifuged for 15 minutes at ≥3 000 rpm. A 10 µL DNase I stock solution (prepared in RNase-free water) was incubated with 70 µL Buffer RDD at room temperature for 15 minutes, mixed by gentle inversion of the tube followed by brief centrifugation. A DNase I incubation mix (80 µL) was added directly to the RNeasy column membrane and placed on a benchtop (20-30°C) for 15 minutes. After incubation, 350 µL Buffer RW1 was transferred to RNeasy column followed by centrifugation at ≥3 000 rpm for 15 s and the flow through was discarded.

3.12.3 RNA purification

A 500 µL Buffer RPE was added to the RNeasy spin column and centrifuged for 15 s at ≥3 000 rpm, and the flow-through was discarded. The RNeasy spin column was placed in a new 1.5 mL collection tube and 50 µL RNase-free water was added directly to the spin column membrane and centrifuged for 1 minute at ≥3 000 rpm to elute the RNA.

3.12.4. cDNA synthesis

The cDNA was synthesized using the RT^2 first strand kit according to manufacturer's instruction. The reagents of the RT^2 First Strand Kit were firstly thawed and centrifuged for 10–15 sec to bring the contents to the bottom of the tubes. The genomic DNA was eliminated by adding 2 µL buffer GE and RNase free water to the RNA. The genomic DNA elimination mix was then incubated for 5 minutes at 42°C and, after incubation, the mixture was immediately placed on ice for 1 minute. A 10 µL reverse transcription mix was added to each tube containing 10 µL genomic DNA elimination mix and mixed gently by pipetting. The mixture was incubated at 42°C for 15 minutes and then the reaction was stopped immediately by incubation at 95°C for 5 minutes. A 91 µL RNase-free water added to each reaction.

3.12.5 Real-Time PCR based array analysis.

The Human Apoptosis RT^2 Profiler PCR Array was used according to the manufacturer's specifications (Qiagen, USA) to profile the expression of 84 key genes involved in programmed cell death or apoptosis. The first step RT^2 SYBR green Mastermix was centrifuged for 10-15 s to bring the contents to the bottom of the tube and the PCR components were prepared for a 96 well plate by adding 1350 µL 2x RT^2 SYBR Green Mastermix, 102 µL cDNA synthesis reaction and 1248 µL RNase-free water to a total volume of 2700 µL. The PCR components were then dispensed into the RT^2 Profiler PCR Array at a volume of 25 µL per well and the plate was tightly closed with adhesive film. The qPCR was run on the Applied Biosystems (ABI) 7500 following the RT^2 Profiler PCR Array protocol under the following conditions: HotStart DNA Taq polymerase activation by incubation at 95°C for 10 minutes. This was followed by 40 cycles of 15 s and 1 minute at 95°C and 60°C cycling conditions respectively. The array has five housekeeping genes (Actb, B2m, Hprt1, Ldha and Rplp1). The microarray data were normalised against the housekeeping genes by the calculation of the change in C_t for each gene of interest. The scatter plot, volcano plot and fold changes of the genes expression were generated using the web portal 3.5 and the results were analysed.

Table 1 1**.** Volumes of Buffer RLT for sample disruption and homogenization

Sample	**Amount**	**Dish**	**Buffer RLT**	**Disruption and homogenization**
Animal cells	$<5 \times 10^6$ $\leq 1 \times 10^7$	<6 cm 6-10 cm	350 µL 600 µL	Add Buffer RLT, vortex (1×10^5 cells); or use QIA shredder, Tissue Ruptor, or needle or syringe
Animal tissues	<20 mg ≤30 mg	- -	350 µL 600 µL	TissueLyser LT; Tissue Lyser II; Tissue Ruptor; or motor and pestle followed by QIA shredder or needle and syringe

3.13 STATISTICAL ANALYSIS

All experiments, except the human apoptosis RT² Profiler™ PCR Array, were performed in triplicate. Data were analysed by GraphPad Prism version 6.0 and GraphPad Instat version 3.06 software. The statistical significance of the results were tested using One-way Analysis of Variance (ANOVA) employing the Turkey-Kramer multiple comparison test between the control and different treatment groups and between treatment groups. RT² Profiler™ PCR Array data were analysed using Qiagen Gene Globe Analyser. Scatter and multigroup plots were generated with the fold change of regulated genes.

CHAPTER 4. RESULTS

4.1 Percentage yield of plant extracts

The percentage yield of the total mass extracted from roots and leaves of *S. italica,* was measured, using two solvents of different polarity, methanol and ethyl acetate. The extraction results of plant material, at a ratio of 1 g extract in 10 mL of solvent using the maceration method, is presented in Figure 4.1. Methanol and ethyl acetate extracted the highest yield in the leaves and the least in the roots, respectively.

Figure 4.1: The total percentage yield of *S. italica* leaves and roots extracted with methanol and ethyl acetate solvents. Methanol and ethyl acetate extracted the highest yield in the leaves (37% and 17%) and least in roots (12.5% and 2.5%), respectively.

4.2 Qualitative analysis of phytochemicals and UV-stable compounds on thin layer chromatography

The plates were developed in mobile phases of varying polarities: TEA, toluene/ethyl acetate/ammonium hydroxide (18:2:0.2) non-polar, CEF, chloroform/ethyl acetate/formic acid (10:8:2) intermediate, and EMW, ethyl acetate/methanol/water non-polar (10:1.35:1). The stable phytocompounds with an affinity for silica gel were observed on thin layer chromatography (TLC) under ultraviolet (UV)-light at different wavelengths of 254 and 365 nm. Different phytochemicals fluoresced in different

colours. At a wavelength of 254 nm, the SIL-EA and SIL-Met extracts at the non-polar mobile phase (TEA) indicated a good resolution. More compounds were indicated by different colours following the polar mobile phase (EMW), and less resolution was observed at the intermediate phase (CEF). In SIR-EA and SIR-Met extract chromatograms, there was a good separation in the intermediate mobile phase (CEF), followed by the polar mobile face (EMW) and only a few separations in the non-polar mobile phase (TEA). At a longer wavelength of 365 nm in Figure 4.2 (Bottom), there were more fluorescent compounds in SIL-EA and SIL-Met as compared to the few compounds indicated by the black bands in SIR-EA and SIR-MET extracts. However, not all compounds fluoresced under the UV-light, so the plates were sprayed with vanillin/sulphuric acid and p-anisaldehyde for the detection of different phytochemicals. The results in Figure 4.3 (upper) show a good separation of different compounds in the polar mobile phases of both SIL-EA, SIL-Met, SIR-EA and-Met extracts after spraying the plates with the vanillin/sulphuric reagent. In SIL-EA and SIL-MET (Figure 4.3, bottom), after spraying with the p-anisaldehyde, there was only a few compounds shown by the black spot. On the other hand, there was better separation in the SIR-EA and SIR-Met depicted by more bands as compared to that of SIL-EA and SIL-Met extracts. However, the overall results indicate that the vanillin/sulphuric reagent gave a better resolution of phytochemicals in all extracts as compared to the p-anisaldehyde reagent spray.

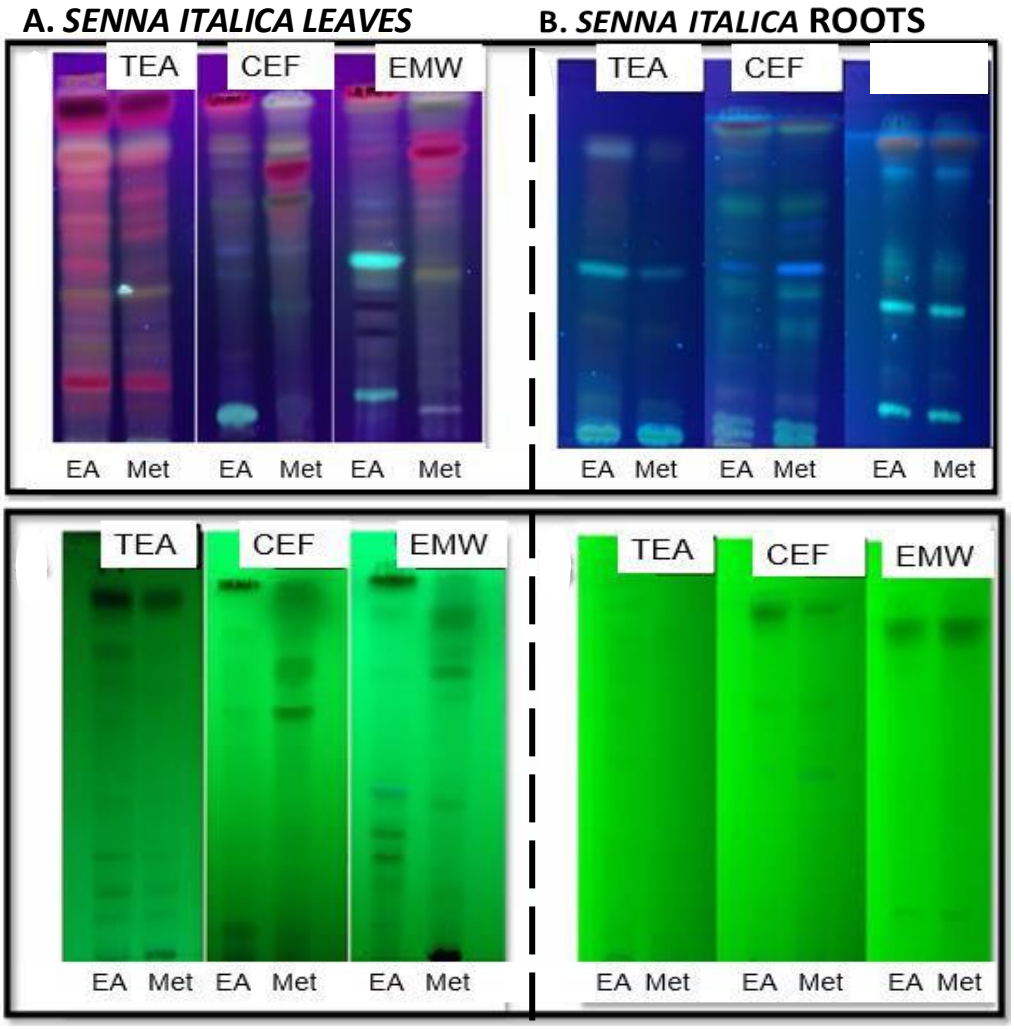

Figure 4.2: **The ultraviolet light fingerprint of *S. italica* (A) leaves and (B) roots**. The plant material was extracted with ethyl acetate (EA) and methanol (Met) solvents. Chromatograms were developed in mobile phases of varying polarities and viewed at wavelengths of 365 nm (Upper quadrants) and 254 nm (lower quadrants).

A. *SENNA ITALICA* LEAVES **B. *SENNA ITALICA* ROOTS**

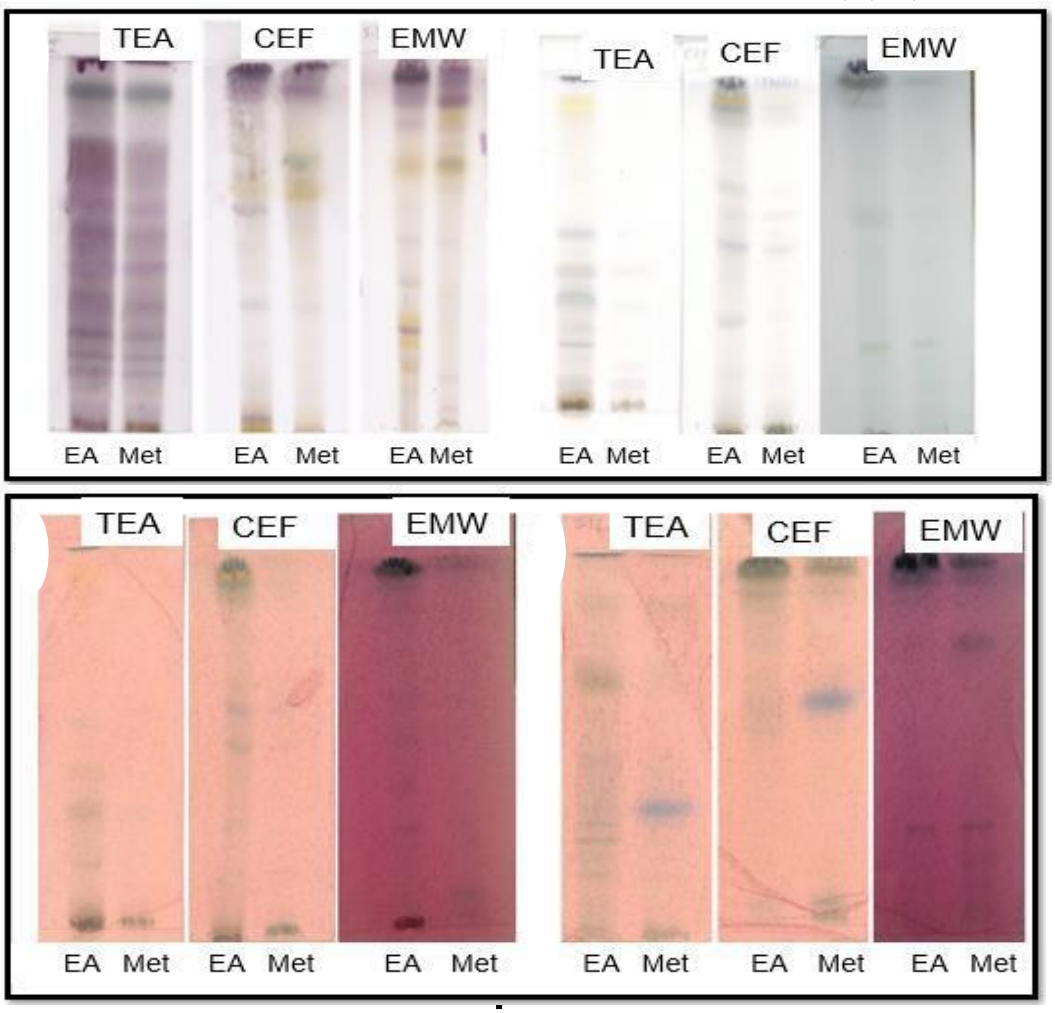

Figure 4. 3: **The fingerprint profile of *S. italica* (A) leaves and (B) roots**. The plant material was extracted with ethyl acetate (EA) and methanol (Met) solvents. Chromatograms were developed in mobile phases of varying polarities and sprayed with vanillin/H_2SO_4 (upper quadrants) and p-anisaldehyde (lower quadrants).

4.3 Qualitative tests for secondary metabolites

The test for the presence of different secondary metabolites was performed on the SIL-EA, SIL-Met, SIR-EA and SIR-Met extracts. The presence of secondary metabolites tannins, flavonoids, terpenoids, steroids and phenols, using different colours as positive indicators, are presented in Table 4.1. In all extracts, there were few steroids and an abundance of all other metabolites. The presence of tannins was indicated by white precipitation; flavonoids by an intense yellow colour which becomes colourless after addition of a dilute acid; terpenoids by deep red coloration; steroids by the reddish-brown colouration ring at the junction and phenols were indicated by the formation of a bluish colour.

Table 4 1. The phytochemical constituent's analysis of SIL-EA, SIL-Met, SIR-EA and SIR-Met extracts.

.

Secondary Metabolites	SIL-EA	SIL-Met	SIR-EA	SIR-Met
Tannins	++	++	++	++
Flavonoids	++	++	++	++
Terpenoids	++	++	++	++
Steroids	+	+	+	+
Phenols	++	++	++	++

Key: Present (+) and strongly present (++), SIL (*Senna italica* leaves), SIR (*Senna italica* roots), EA (Ethyl acetate), Met (Methanol).

4.4 Quantitative phytochemical analysis

The total phenolic and flavonoid content of the extracts was determined using the gallic acid and quercetin equivalence assays, respectively. The results were determined by linear regression from the standard curve. Tannic acid is known as one of the high phenolic compounds and quercetin as one of the natural flavanols found in the plants. They were used as reference points for phenolic and flavonoid content. The results in Figure 4.4 and Table 4.2 show high phenolic content in the SIL-Met extract (13,6 ± 0,35) and the least in the SIR-EA extract (1,1 ± 0,20). High flavonoid content was observed in the SIR-EA extract (12,16 ± 0,44) and less in the SIL-Met (4,16 ± 0,35) extract.

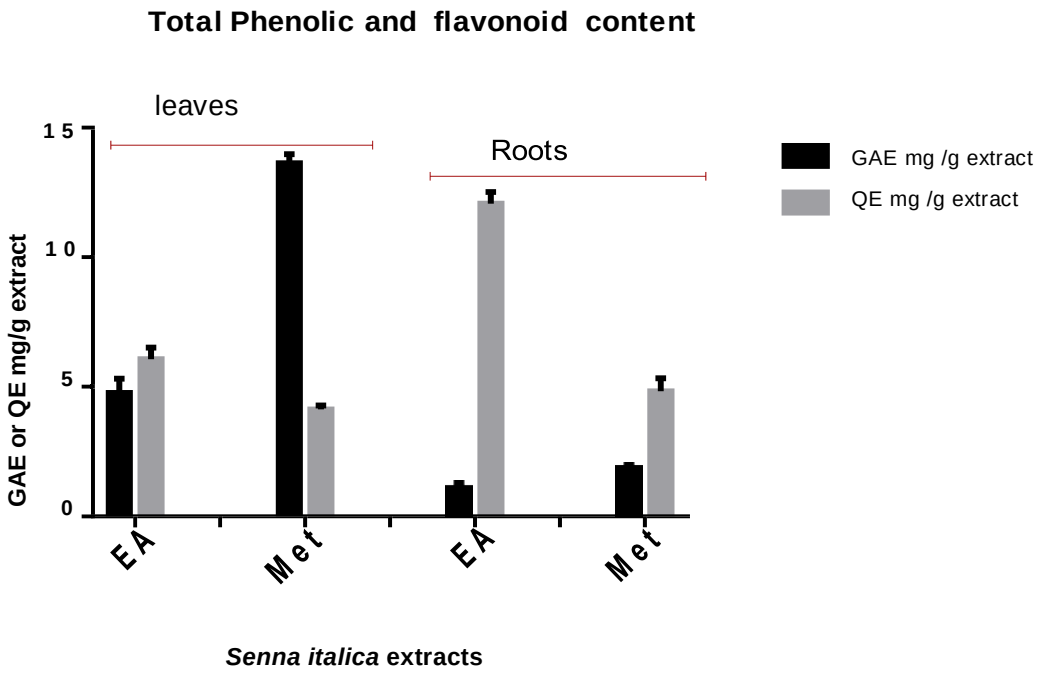

Figure 4. 4: **The total phenolic content of *S. italica* methanol and ethyl acetate crude extracts**. The results were expressed as Gallic acid equivalents (GAE mg/g) and flavonoids content expressed as quercetin equivalent (QE mg/g). *Senna italica* EA (Ethyl acetate) and Met (Methanol).

Table 4 2. Quantitative analysis of the chemical constituents of *Senna italica* leaves and roots extracts.

Extract	Total phenolic compounds, (mg/g)	Total flavonoids compounds, (mg/g)
SIL-EA	4,8 ± 0,55	6,1 ± 0,43
SIL-Met	13,6 ± 0,35	4,16 ± 0,35
SIR-EA	1,1 ± 0,20	12,16 ± 0,44
SIR-Met	1,9 ± 0,12	4,19 ± 0,16

Key: Sir (*Senna italica* roots), Sil (*Senna italica* leaves), EA (Ethyl acetate) and Met (Methanol)

4.5 Antioxidant analysis

4.5.1 Qualitative antioxidant analysis

The antioxidant potential of *S. italica* was determined by spraying plates with 0.2% DPPH dissolved in methanol. The chromatograms were developed in mobile phases of varying polarities, ranging from non-polar to polar i.e. TEA, CEF and EMW. The intense yellow band in the purple background in plates sprayed with DPPH shows the presence of antioxidant compounds in the extract. The chromatogram for *S. italica* roots in the TEA non-polar mobile phase, relative to the leaves chromatogram in the same solvent system, showed a high intensity band of yellow. In the CEF mobile phase, the roots and leaves extracts indicated a good resolution of antioxidants denoted by an intense yellow band. However, poor separation was observed in the polar mobile phase (EMW) for both leaves and roots extracts as indicated by light yellow bands.

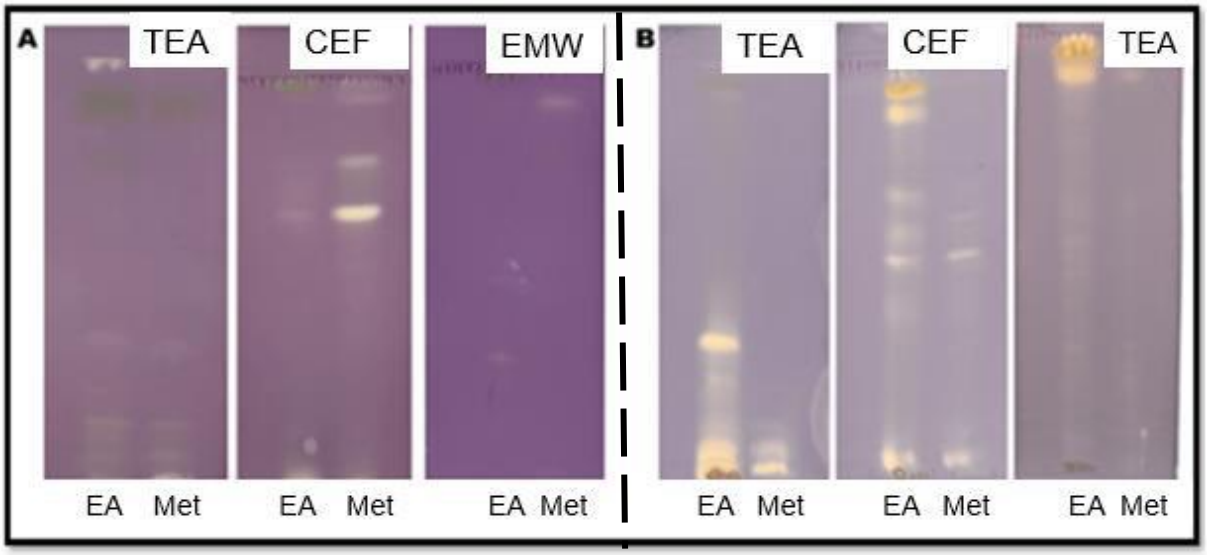

Figure 4. 5: ***Senna italica* antioxidant activity.** Antioxidant potential of *S. italica* (A) leaves and (B) roots EA (Ethyl acetate) and Met (Methanol) extracts on TLC plates developed in varying polarities mobile phases, TEA, CEF and EMW. The chromatograms were sprayed with 0.2 % of DPPH dissolved in methanol.

4.5.2 Quantitative antioxidant analysis

4.5.2.1 DPPH scavenging assay

The different concentrations of *S. italica* extracts were prepared (0 to 1000 µg/mL) and similar concentrations of ascorbic acid were also prepared and used as a positive control based on its higher scavenging potential. The SIL-Met extract showed a higher scavenging activity at concentrations of 500 µg/ml and 1000 µg/ml as compared to ascorbic acid at the same concentrations. The SIR-EA extract exhibited the lowest DPPH scavenging potential activity at all concentrations. The ferric ion reducing power assay is a method based on the presence of the potential agent or antioxidant in the extract to reduce ferric ions into ferrous ions forming a blue colour. All *S. italica* extracts exhibited a less reducing power compared to ascorbic acid.

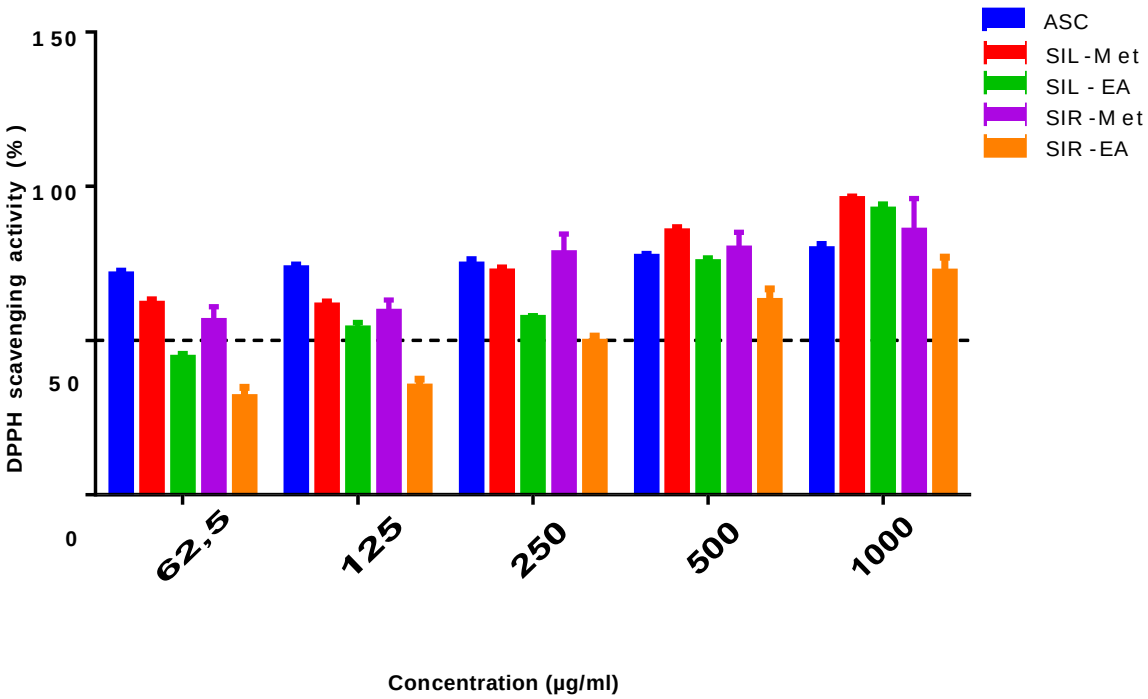

Figure 4. 6: ***Senna italica* quantitative DPPH antioxidant activity analysis**. The percentage of the DPPH free radicals that are scavenged by different concentrations of *Senna italica* roots and leaves extracts. Ascorbic acid was used as a positive control. ASC (Ascorbic acid), SIL (*Senna italica* leaves), SIR (*Senna italica* roots), Met (Methanol) and EA (Ethyl acetate).

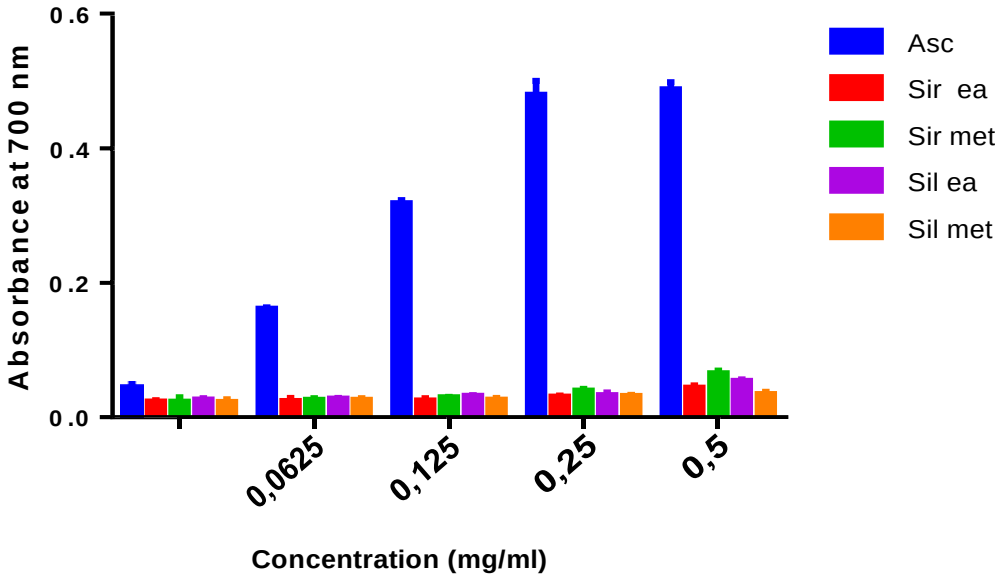

Figure 4. 7: **The reducing power potential of *S. italica* extracts**. The ferric ion percentage reduced by different concentrations of *S. italica* roots and leaves extracts. Ascorbic acid was used as a positive control. ASC (Ascorbic acid), SIL (*Senna italica* leaves), SIR (*Senna italica* roots), Met (Methanol) and EA (Ethyl acetate).

4.6. The cytotoxic effect of *S. italica* leaves and roots extracts in A549 lung cancer cells

The cytotoxic effect of different concentrations (200 µg/ml to 800 µg/ml) of ethyl acetate and methanol *S. italica* leaves and roots extracts was determined using MTT assay following 24 hrs of treatment. The DMSO served as a negative control and 70 µM of curcumin served as a positive control. The results in Figures 4.10A and B show that 200 µg/ml of SIR-EA extract inhibited 50% of viable cells. Both the methanol roots and leaves extracts enhanced the viability of treated cells in comparison to the untreated cells, instead of inhibiting viability (figure 4.10A). The potential and ability of the SIR-EA to be selectively cytotoxic were tested using the Hek-293 cells and data shows that a higher percentage of cells were viable at 100 µg/ml as compared to 200 µg/ml (figure 4.10B). The results in figure 4.11A show that the root ethyl acetate extract has no cytotoxic effect against the normal kidney cells Hek-293 using MTT assay. The MTT results were further confirmed using cell viability and dead cell count assays and the results show no effect of the extract on the normal cells.

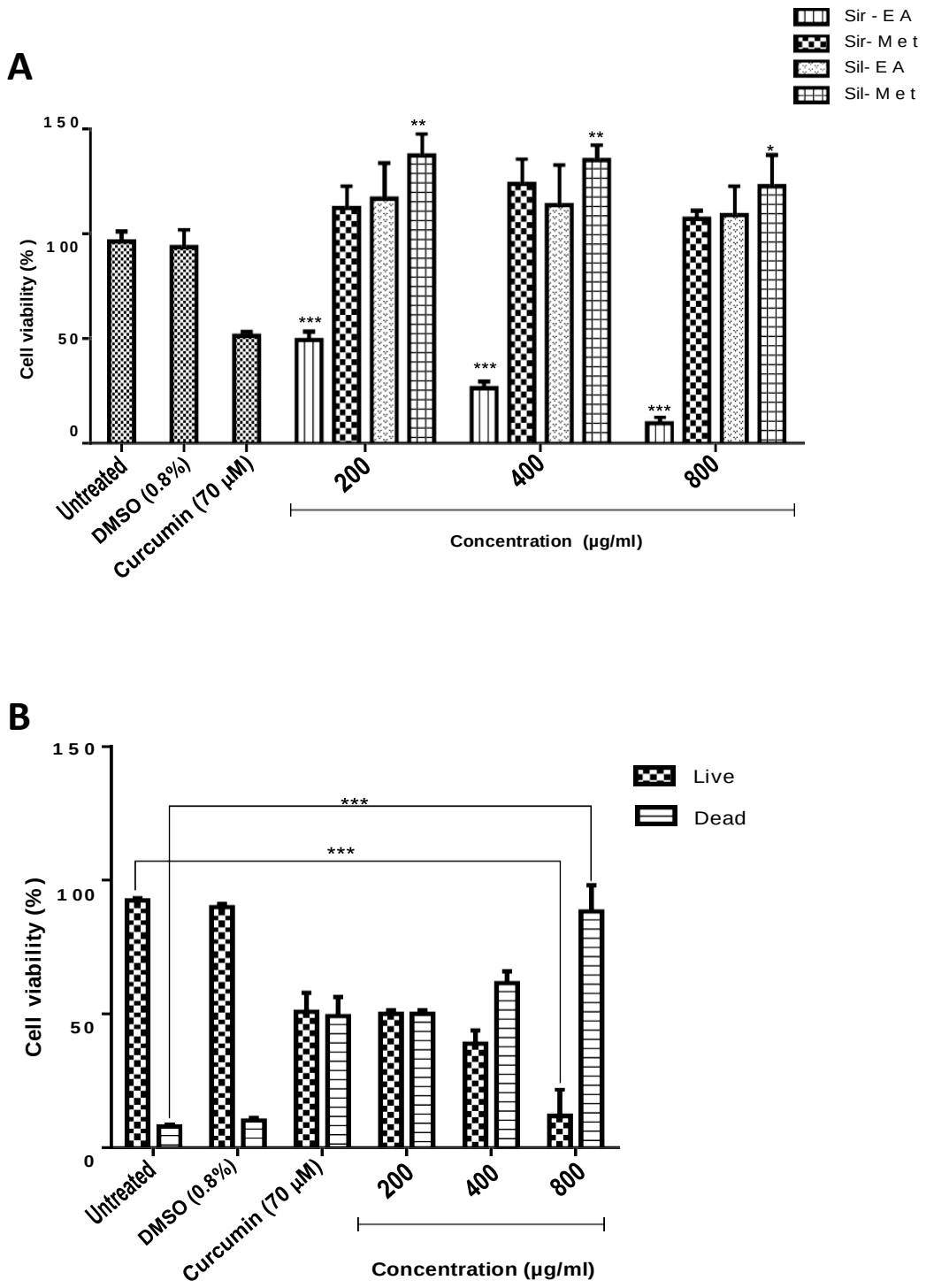

Figure 4. 8: **Cytotoxicity effect of *S. italica* extracts in A549 lung cancer cells.** (A) Cells were treated with different concentrations of ethyl acetate and methanol extracts for 24 h and cytotoxicity were analysed using MTT assay and (B) cytotoxicity of ethyl acetate root extract confirmed using cell viability and dead cell count assay. Data is of three independent experiments (percentage mean ± SEM). *p < 0.05, **p < 0.01, ***p < 0.001.

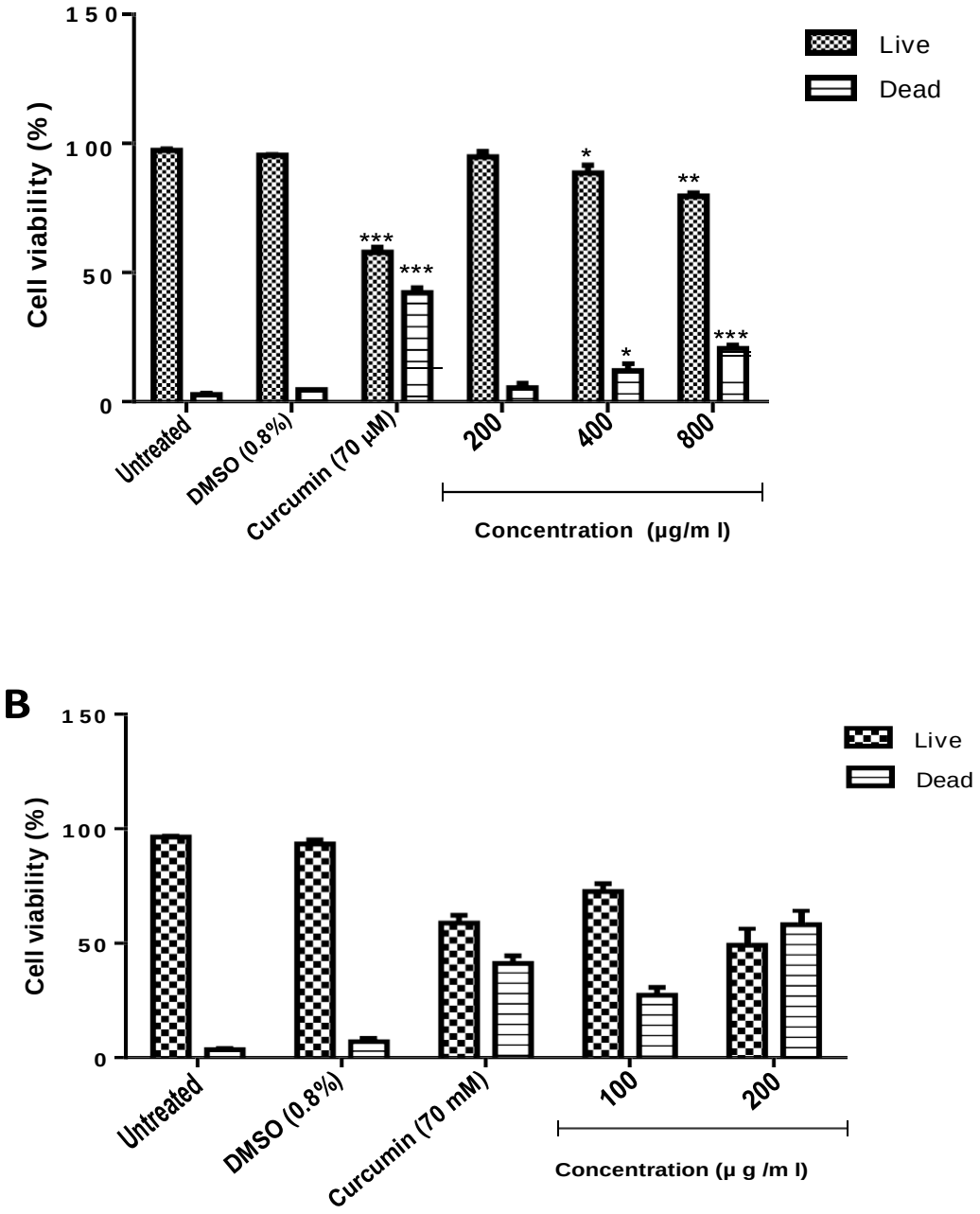

Figure 4. 9: **Cytotoxicity effect of *S. italica* extracts in HEK-293 cells** (A) Cell viability and dead cell count of lung A549 cancer cells treated with different concentrations of the methanol root extract of *S. italica* for 24 h and (B) Cell viability and dead cell count of HEK-293 cells treated with different concentrations of the ethyl acetate root extract of *S. italica* for 24 h. Data is of three independent experiments (percentage mean ± SEM). *p < 0.05, **p < 0.01, ***p < 0.001.

4.7. The effect of ethyl acetate root extract on the proliferation and DNA damage potential of the A549 lung cancer cells.

The effect of SIR-EA extract on the proliferation of A549 lung cancer cells was assessed using the Ki67 proliferation assay. Figure 4.12 shows that, in untreated cells, about 90 % of the total cells were proliferating and 70 µM curcumin reduced proliferation by 45%. Ethyl acetate roots extract (100 µg/ml and 200 µg/ml) reduced proliferation by 41% and 46%, respectively. There was no phosphorylation of either ATM or H2AX in untreated cells. On the other hand, the SIR-EA extract induced genotoxicity, resulting in statistically increased levels of ATM phosphorylation but not H2AX phosphorylation (Figure 4.13). Curcumin treated cells resulted in increased levels of ATM but not H2AX phosphorylation.

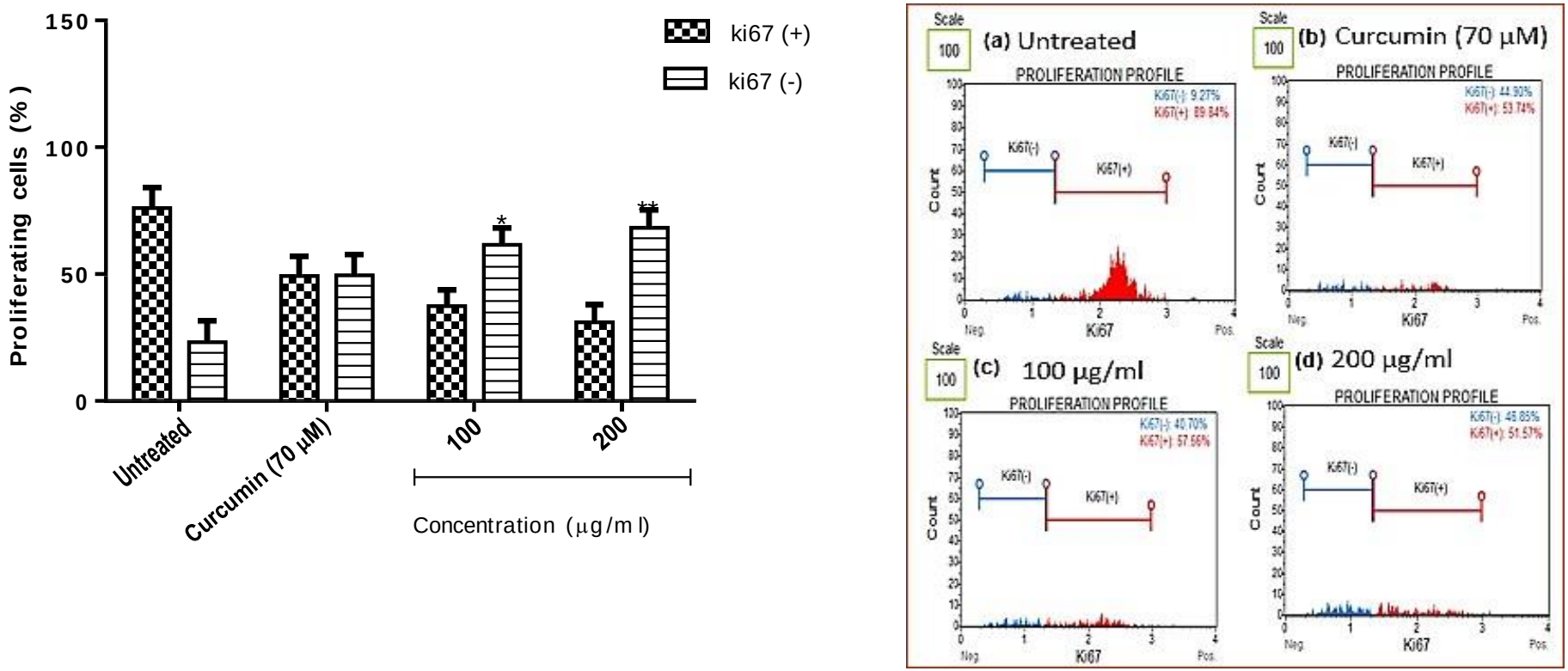

Figure 4. 10: **The proliferation of lung A549 cancer cells.** Cells were treated with different concentrations of the ethyl acetate root extract of *S. italica* for 24h. Data is a representation of three independent experiments (percentage mean ± SEM). *p < 0.05, **p < 0.01.

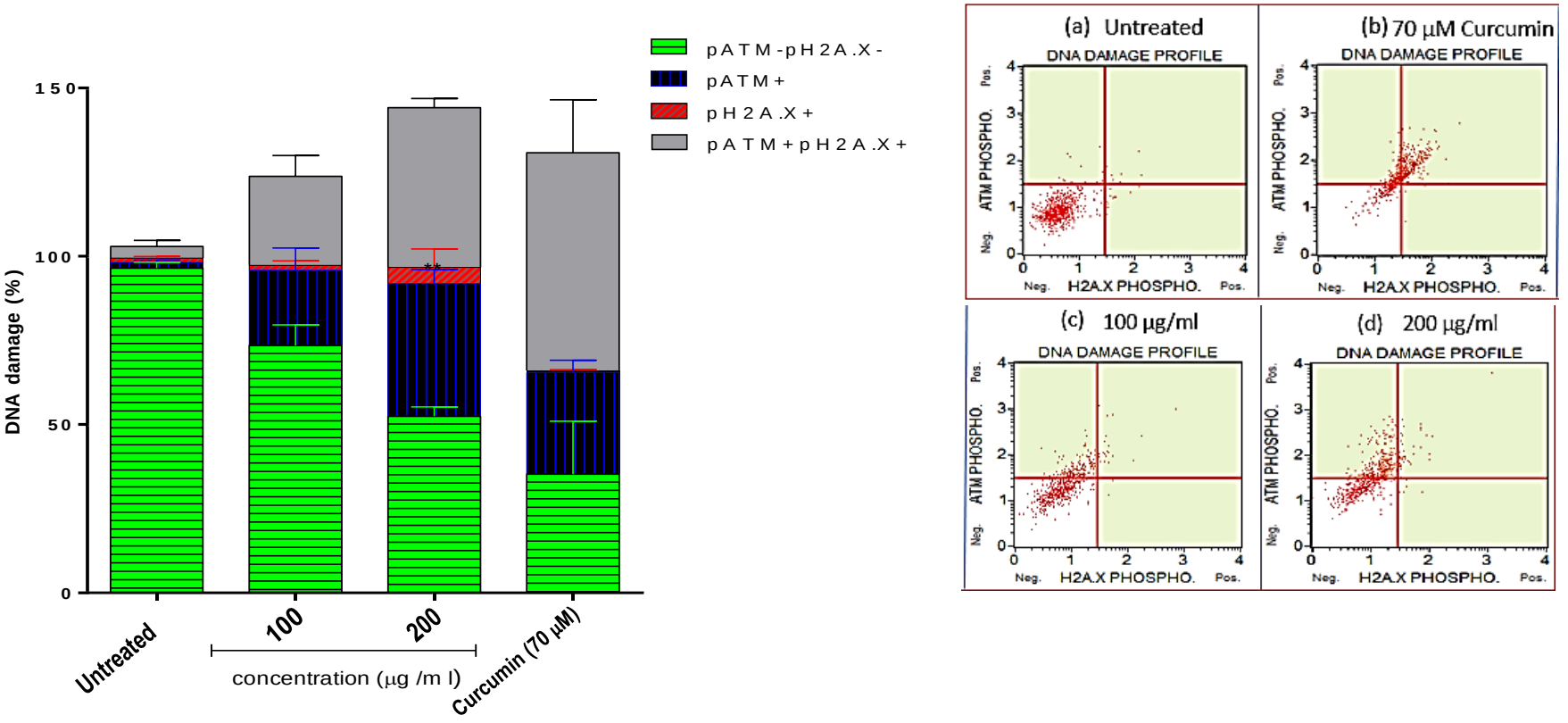

Figure 4. 11: **DNA damage response in lung A549 cancer cells**. The cells were treated with different concentrations of the ethyl acetate root extract of *S. italica* for 24 hours. Data is a representation of three independent experiments (percentage mean ± SEM). **p < 0.01.

4.8 The apoptosis assessment of ethyl acetate roots extract in A549 lung treated cells.

The apoptosis features were analysed using acridine orange/ethidium bromide dual staining. The red colour is an indicator of apoptotic cell death and the green colour is an indicator of viable cells. The results in Figure 4.13 show the morphological and apoptotic features on the lung A549 cancer cells after 24 hrs treatment with the positive control (70 µM curcumin) and ethyl acetate root extract. The total live cells were over 75% in both treated and untreated cells. The positive control curcumin had 15.65% of cells in the early apoptosis phase. The SIR-EA extract at 100 µg/ml and 200 µg/ml depicted a few cells undergoing early apoptosis with a percentage of 4.85% and 2.95%, respectively. Only few cells were undergoing late apoptosis: untreated cells (3.90%), 70 µM curcumin (6.40%), 100 µg/ml (6.35%) and 200 µg/ml (9.30%). The total apoptotic cells were higher in the positive control (70 µM curcumin) and less at 200 µg/ml and 100 µg/ml.

4.9 RT^2 PCR array identification of the apoptosis pathway

The results in Figure 4.15 show 84 key genes that are involved in apoptosis represented in a scatter plot. The scatter plot shows the expression of genes analysed after the treatment of A549 cancer cells with the SIR-EA extract. The results in Table 4.3 show the expressed genes average C_t value and also the fold change as compared to the control. A sum of 9 genes out of 84 was found to be upregulated.

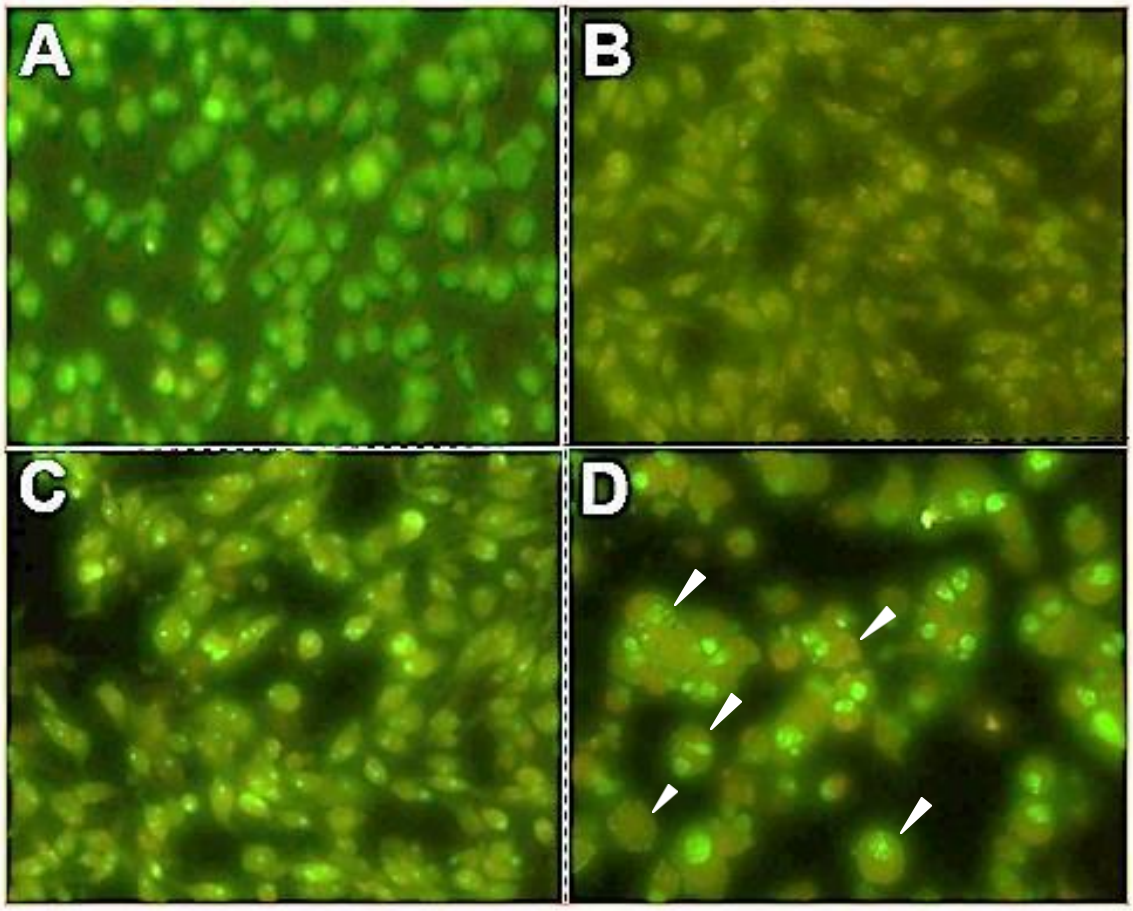

Figure 4. 12: **The morphological features following treatment with dual stains.** The lung A549 cancer cells were treated with different concentrations of the ethyl acetate root extract of *S. italica*. (A) Untreated, Curcumin 70 µM (B), 100 µg/ml (C) and 200 µg/ml (D), Curcumin (B) were stained with acridine orange/ ethidium bromide double stain. The white arrows indicate nuclear fragmentation.

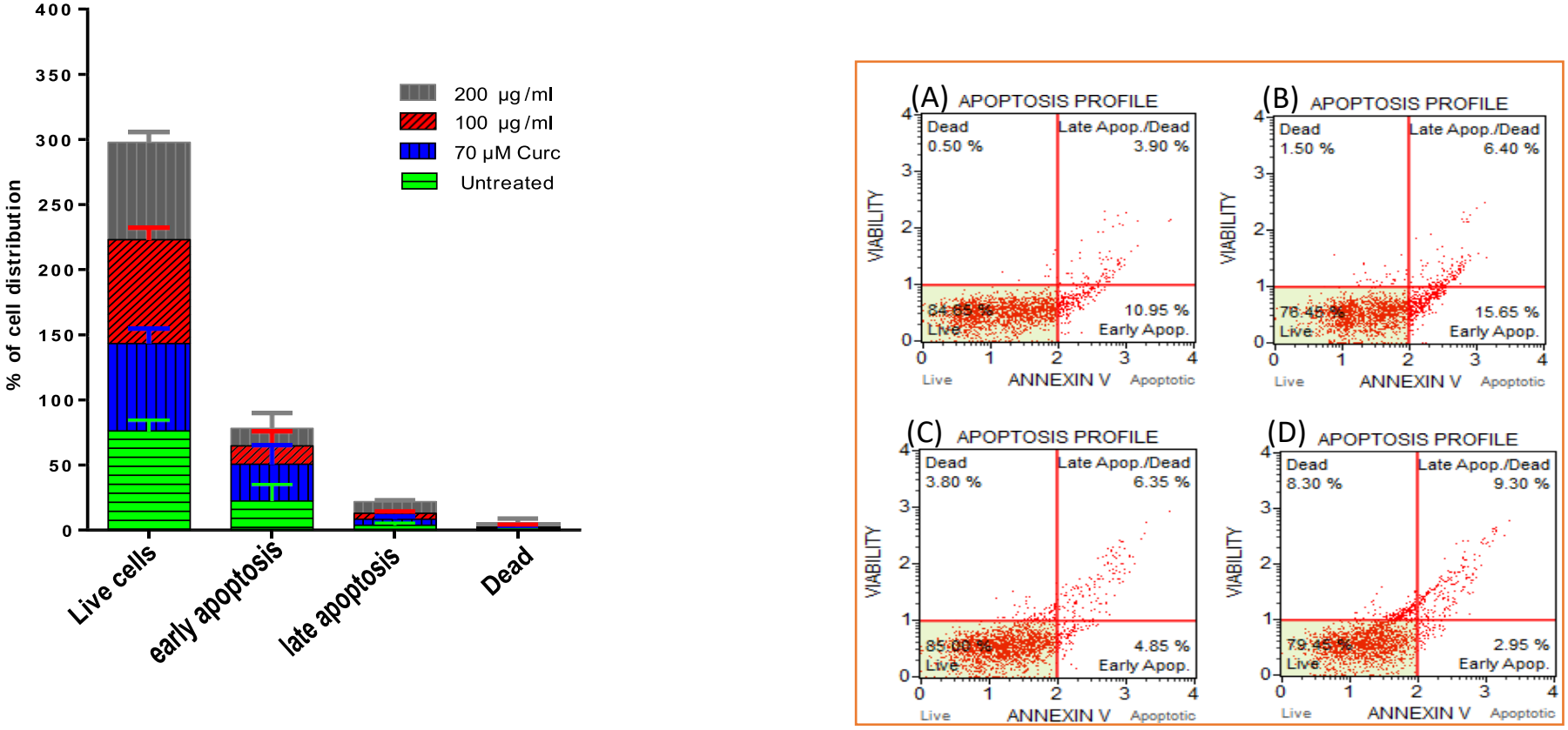

Figure 4. 13: **The evaluation of apoptosis induction in lung A549 cells using Annexin V/dead cell assay.** The A549 cells were treated with (A) Untreated, Curcumin 70 µM (B), 100 µg/ml (C) and 200 µg/ml (D) for 24 hrs and the apoptosis features were assayed using flow cytometry. Curcumin was used as a positive control with the untreated cells as a negative control. The flow cytometry was carried out using the Muse cell analyser.

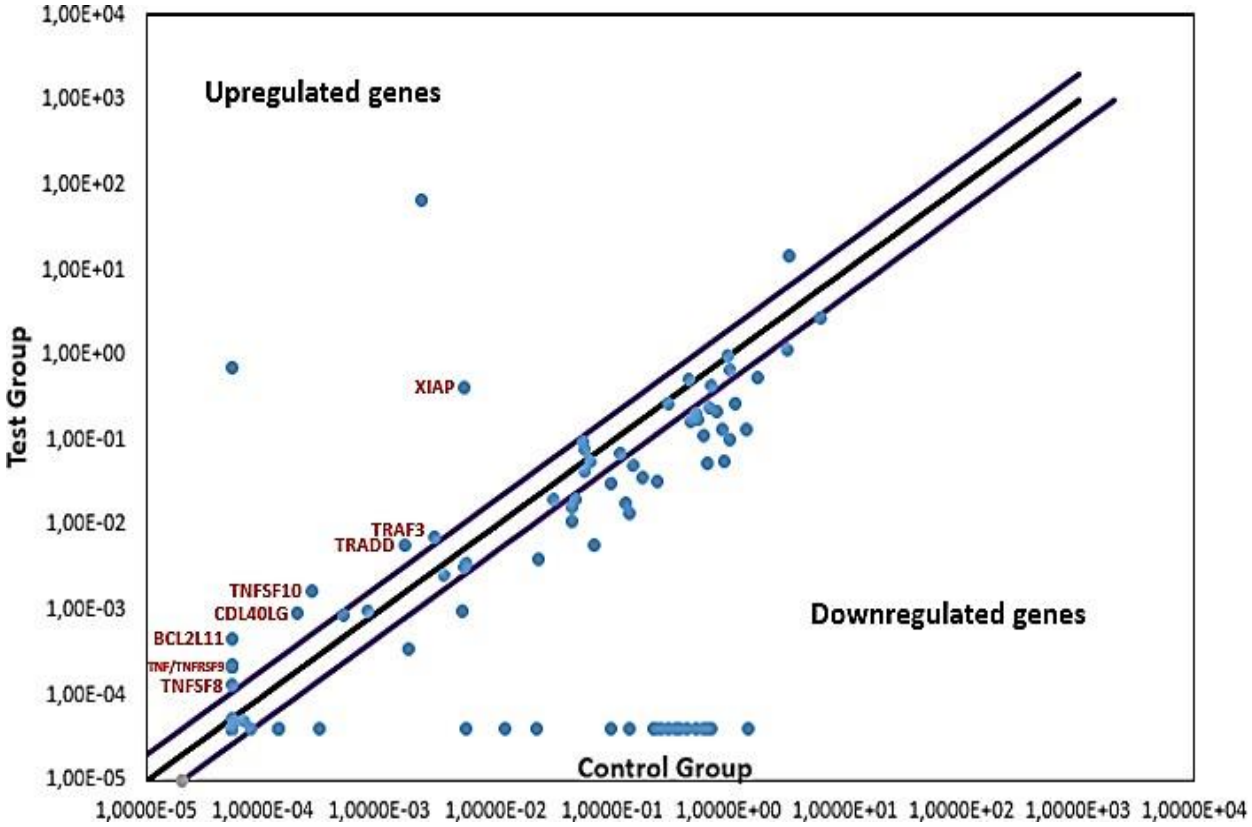

Figure 4. 14: The Scatterplot of qPCR array results. The results depict the effect of *Senna italica* root extract on the A549 lung cancer cells. The total RNA was extracted after 24h treatment and it was reverse transcribed into cDNA, followed by the analysis using the commercial 384-well plate SYBR. PCR array that profiles 84 pathway-focused key genes involved in apoptosis.

Table 4 3. Changes in relative expression for cancer related genes between the 200 µg/ml *S. italica* root ethyl acetate treated and untreated A549 cells.

Gene	Fold change	Average Raw CT	
	treated/untreated	Untreated cells	Extract treated cells
CIDEB	-7.21	23.74	26.13
TP53	-3.24	19.99	21.22
TNFSF8	2.47	35.00	33.23
TNF	4.18	35.00	32.47
DIABLO	-2.74	19.18	20.17
TNFRSF9	3.84	35.00	32.59
BCL2L11	8.52	35.00	31.44
CDL40LG	4.66	33.15	30.46
TNFSF10	6.52	32.74	29.57
TRADD	3.56	30.07	27.77
TRAF3	2.31	29.20	27.53
XIAP	79.61	28.40	21.62

4.10. GRAPHICAL SUMMARY OF RESULTS

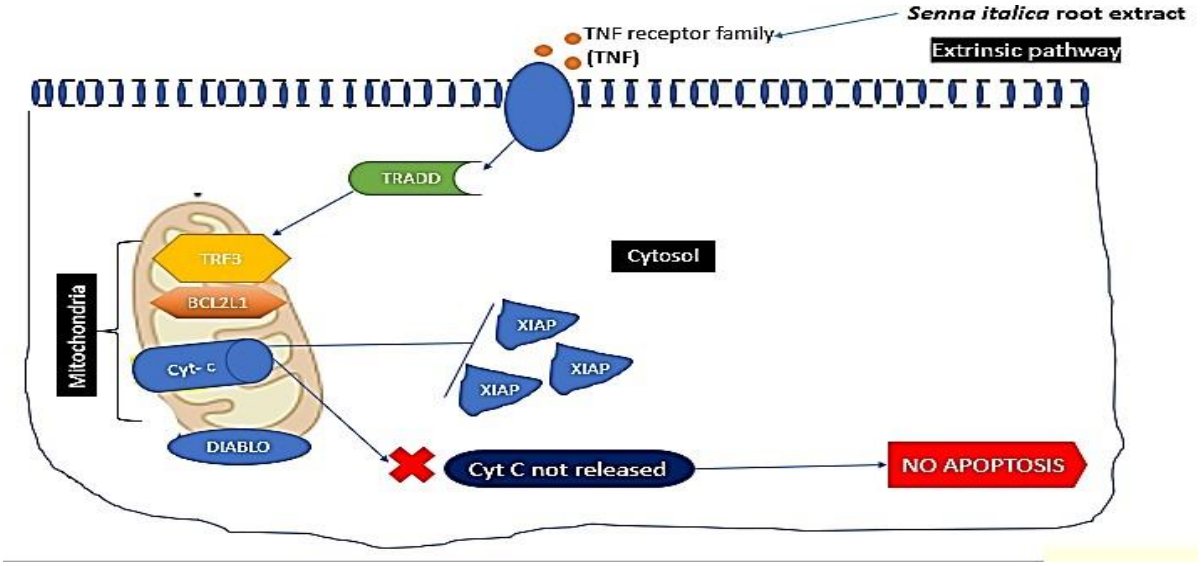

Figure 4.15: Proposed molecular mechanism of action of the *Senna italica* ethyl acetate root extract. The *Senna italica* root extract activates the TNF-receptor mediated pathway and high XIAP prevents the release of cytochrome C, resulting in the inactivation of apoptosis.

CHAPTER 5: DISCUSSION AND CONCLUSION

Lung cancer remains one of the cancers that cause a higher mortality rate worldwide in both males and females. The incidences are expected to increase in the future despite the available treatments and these high incidences are mostly attributed to the change of lifestyle and continued industrialisation in developing countries. The continual failure of available treatments is a driving factor of the need for alternative treatment as opposed to the currently available ones.

Worldwide and most people in Africa still depend on traditional medicines for the treatment of various diseases. Various plant parts such as the roots, stems, fruits and leaves are used. The abundance and ready availability of different species of plants give researchers a platform to explore the healing power of different plants. A portion of the total available pharmaceutical drugs (25%) are derived from plants that were reported to be used in traditional medicine first and the plants are known to possess antitumor potential (Sawadogo *et al*., 2012). The study is aimed at determining the differential expression of apoptotic genes induced by treatment with *S. italica* root and leaf extract.

5.1. Phytochemical analysis

5.1.1 The percentage yield of plants extracts

The choice of extractant used to extract different plant materials is influenced by its polarity. Methanol and ethyl acetate were used as extractants of *S. italica* due to their polar nature. Both solvents have varying polarity indexes that gives them the advantage to extract different compounds. The results suggest that methanol, as compared to ethyl acetate, extracted more compounds. This is due to the high polar index of 6.6 for methanol as compared to that of 4.4 for ethyl acetate. Even though ethyl acetate had less % yield, its biphasic property gave it the advantage to extract both the polar and non-polar compounds (Widyawati *et al*., 2014). The results in Figure 4.1 show that methanol had a high extraction yield in both roots and leaves as compared to ethyl acetate. This is due to the smaller molecular weight of methanol which enables it to penetrate the plant material. The results were in agreement with the findings by other researchers which has demonstrated that methanol extract of *S. italica* has a higher percentage yield (Mokgotho *et al*., 2013). Despite different studies showing a higher % yield of methanol, if it is used as extractant, there is no direct

relationship of the extract activity with its percentage yield, and the cytotoxicity in other studies has been demonstrated to be inversely proportional to the percentage yield (Alzeer *et al*., 2014.)

5.2 Qualitative analysis of phytochemicals and UV-stable compounds on thin layer chromatography viewed under UV-light

Thin layer chromatography is a technique often used to determine the presence of different compounds in plant extracts. The compounds present in extracts move on the TLC plates depending on their solubility in the mobile phase used. The compounds that dissolve in a mobile phase move further on a TLC plate while the non-soluble compounds have high affinity with the TLC particles and remain at the bottom of the plate (Bele *et al*., 2011). The method is mostly used because it is versatile, readily available and good in determining the quality of the herbal drugs (Roy *et al*., 2018). The results in Figure 4.2 depict the *S. italica* leaf and root extracts developed in different mobile phases of varying polarities, TEA- nonpolar, CEF-intermediate and EMW- polar mobile phases. The overall results at a longer wavelength of 365 nm show that most of the compounds in the SIL-EA and SIL-Met were non-polar and most of the compounds in the SIR-EA and SIR-Met were intermediate in nature. The results in Figure 4.3 show the presence of compounds that have the potential to quench the green fluorescence light at a shorter wavelength. The results further suggest that the SIL-EA and SIL-Met have a wide range of compounds fluorescing at both short and long wavelengths compared to the SIR-EA and SIR-Met extracts.

5.3 Qualitative tests for secondary metabolites

Some of the different compounds that are found in the plant extracts can be seen with a naked eye while others must be visualised using different reagents solutions. The terpenoids are one of the abundant phytoconstituents found in plants and the presence of terpenoids in plant extracts are indicated by dark green, brown and purple colours (Pascaline *et al*., 2011). Different sprays were used to target different compounds. The results in Figure 4.3 (upper) indicate the presence of steroids, which are non-polar, in the SIL-EA, SIL-Met, SIR-EA and SIR-Met extracts in the presence of vanillin reagent.

The *p*-anisaldehyde is also used to detect the presence of steroids, phenols and terpenes presented by different colours on a TLC plate after heating (Figure 4.3, bottom). The results suggest that there was a higher presence of terpenes, sugars, and phenols in the SIR-EA and SIR-Met extracts as compared to the SIL-EA and SIL-Met extracts. Results from Table 4.1 corroborate the results from Figure 4.3, which indicates an abundance of phenols and terpenoids.

These results were in agreement with the findings by other researchers (Masoko *et al*., 2010) which have shown that *S. italica* has different compounds that differ in polarity. The results further suggest that the vanillin/sulphuric acid assay, as compared to p-anisaldehyde assay, demonstrated good separation of the UV-stable compounds.

5.4 The quantitative analysis of the *Senna italica* phytochemicals

The phenolic compounds are known to be abundant in plants since most of the secondary metabolites are derivatives of phenolic compounds. They have various properties such as anticarcinogenic, antiaging, cardiovascular protection and inhibition of cell proliferation. Most of the medicinal plants with antioxidant properties have been reported to have higher phenolic compounds (Vaghasiya *et al*., 2011). The medicinal plants are also known to have phenolic compounds in the form of flavonoids, which are reported to have various health benefits when consumed. The results in Figure 4.4 shows the phenolic and flavonoid contents of ethyl acetate and methanol root and leaf extracts. The overall results of leaf compared to root extracts shows that methanol leaf extract has the highest concentration of phenolics as compared to all extracts, and ethyl acetate root extract has the highest concentration of flavonoids as compared to all other extracts

5.5 Antioxidant analysis

Antioxidants are substances that inhibit oxidative damage. There are natural antioxidants found in different plants and synthetic ones. The natural antioxidants are preferred for different drug development and they are known to have various health benefits due to their ability to prevent oxidation which occurs in the proteins, DNA or lipids (Labiad *et al*, 2014). Free radicals, like hydroperoxide, lipid peroxyl or hydroperoxide, are continuously produced by the body, and they contribute to the cause of different diseases. They are scavenged by antioxidants such as flavonoids, polyphenols and phenolic acids (Mahdi-Pour *et al*., 2012). The higher phenolic content

in the SIL-MET extract in Figure 4.4 has contributed to the antioxidant activity of the SIL-MET extract depicted by yellow spots on the TLC plate, against the purple background of DPPH in Figure 4.5. These results correspond with the findings by Piluzza *et al*. (2011) which show that higher phenolic content contributes to the total antioxidant present in an extract. The SIR-EA extract has a higher flavonoid content with low phenolic content as compared to the SIL-EA extracts. The SIR-EA extract had an overall good separation of antioxidants as indicated by yellow spots in Figure 4.5.

The quantitative estimation of the activity of antioxidants from plant extracts is determined using different assays because the antioxidant activity in plant extracts occurs through different mechanisms. It is difficult to determine the antioxidant activity of an extract using only one assay (El Jemli *et al*., 2016). The first assay that was used to determine the quantity of antioxidants in this study was the DPPH assay, which is based on a stable free radical DPPH which is reduced into DPPH-H (Jothi *et al*., 2015). The second assay used was the iron reducing power of the extract from ferric ion (Fe^{3+}) to ferrous ion state (Fe^{2+}) assay, which is one of the reproducible methods used in the estimation of antioxidants in extracts. The results in Figure 4.6 depict a good radical scavenging power of SIL-MET in a concentration dependant manner as compared to all three extracts (SIL-EA, SIR-MET and SIL-EA). The SIL-MET, as compared to the positive control, has a higher inhibition potential as compared to ascorbic acid. The SIR-EA extract has a lower inhibition activity at all concentrations as compared to all other extracts and these results are in correlation with the results obtained in Figure 4.4 of total phenolic content. The higher phenolic content contributes to higher scavenging activity of SIL-Met extract as compared to lower scavenging activity of SIR-EA extract due to the lower phenolic content. The results in Figure 4.7 show a low ferric ion reducing power by all four extracts as compared to ascorbic acid, which shows a very high reducing power in a concentration dependent manner. The two assays have shown the presence of antioxidants in extracts and the DPPH assay displayed a very good determination of antioxidant. The *S. italica* plant extracts has shown the presence of antioxidants which are known to play a pivotal role in treatment of various diseases such as cancer, gastric problems and heart failure (Shunmuga Jothi *et al*., 2015).

5.6 The cytotoxic effect of *S. italica* leaf and root extracts in lung A549 cancer cells.

The determination of the cytotoxic and non-cytotoxic effect of plant compounds is an important step in drug development as it measures the quantities that can be harmful to biological components (Drahansky *et al*., 2016; Miret *et al*., 2006). The MTT assay was the first step to determine the IC_{50} of *S. italica* extracts in the lung A549 cancer cells. The MTT assay determines the mitochondrial integrity of cells due to the ability of viable cells to convert the tetrazolium into formazan crystals, and is used to determine the concentration of the drug that decreases the concentration of viable cells by 50% (IC_{50}) (Meerloo *et al*., 2011).

The results in Figure 4.8A show that SIL-EA, SIL-MET and SIR-MET extracts promote the growth of the lung A549 cells instead of inhibiting their viability. The unusual findings of the plant extract that promotes the growth of the cancer cells were also reported by Steenkamp and Gouws (2006). They found that out of the six medicinal plants that they were testing for cytotoxicity against cancer cells, some promoted their growth; however the reason for this effect is unknown. The results of SIR-EA shows that the extract had a cytotoxic effect against the lung A549 cancer cells in a concentration dependant manner with an IC_{50} of 200 µg/ml. The findings of this study were similar to other studies, which show that the ethyl acetate extracts of *S. italica* have anti-cancerous activity against different cancer cell lines: epithelioid carcinoma (Hela), human prostate cancer (PC3), mammary gland breast cancer (MCF-7) and hepatocellular carcinoma (HePG-2).

The results of the ethyl acetate root extract and methanol root extract, obtained using an MTT assay, were confirmed by the cell viability and dead cell count assay; a rapid, simple and linear assay used for viability and concentration of cells. The results of SIR-EA extract in Figure 4.8A showed that SIR-EA reduced viability of A549 cells in a concentration dependent manner and the results in Figure 4.8B also confirm that the root ethyl acetate extract had cytotoxic effects in a concentration dependent manner with an IC_{50} of 200 µg/mL. The methanol leaf and root extracts showed no cytotoxic effect against the lung A549 cancer cells even at higher concentrations (Figure 4.9A). The results in Figure 4.9B show that SIR-EA, when tested against the HEK-293 which served as normal cells, was not toxic with > 70% of cells were viable following 24 hrs of treatment.

5.7 The effect of ethyl acetate root extract on proliferation and DNA damage potential in lung A549 cancer cells

The cancerous cells are forever proliferating as an indication of cell growth. Ki67 is a nuclear protein present in cells that acts as a proliferation marker. Since one of the characteristics of cancerous cells is over proliferation, it is a suitable marker used in cancer studies to quantify the proliferation of the cancerous cells (Dzulkifli *et al*., 2018). The antioxidants present in herbal medicine have been proven over the years to have antiproliferative potential and can exhibit apoptosis in cancerous cells through the activation of apoptotic genes. The results in Figure 4.10 show that 200 µg/ml SIR-EA reduced proliferation of the Ki67 (-) gene in lung A549 cancer cells by >60% as compared to 70 µM curcumin which reduced proliferation by 50%. Curcumin is a derivative of turmeric which has been used over centuries in traditional medicine to treat different diseases and scientifically it has been outlined to have interference on different signalling pathways i.e. apoptosis, cell-cycle regulation and proliferation (Anand *et al*., 2008).

DNA damage potential is one of the mechanisms cancer therapies use to treat different types of cancers. DNA damage occurs because of the cytotoxic agents, which activate the cell cycle checkpoints, leading to cell arrest. Cell death usually follows DNA damage with different proteins responding to DNA damage, one of them being ataxia telangiectasia mutated (ATM), a serine/threonine kinase. The ATM protein is activated by damage in the DNA of cells and, as a result, it phosphorylates different downstream factors and one of those is histone variant H2A.X (Swift and Golsteyn, 2014). The H2A.X is an important indicator of the extent of DNA damage as its increase is equal to the level of DNA damage. The results in Figure 4.11 show that SIR-EA promoted DNA damage and ataxia telangiectasia mutated (ATM) kinase activation of lung cancer cells. However, the increased phosphorylation of H2A.X was not observed and the activation of this histone variant is important since it shows if there is DNA damage and the extent of the damage. Once the damage of DNA increases. H2A.X also increases and accumulates at the site at which the damage is occurring. These results further show that even though there was an activation of ATM, it was not sufficient enough to phosphorylate some of the genes that activate apoptosis such as the p53. The results have further shown that the pro-apoptotic gene, BCL2L11, was upregulated, and is said to be released if there is a toxic stimuli (Luo and Rubinsztein,

2013). The results in Figure 4.11 shows that there was a toxic stimulus of SIR-EA to the lung A549 cells. However the pro-apoptotic genes: *bax*/*bak*, were not upregulated and, as result, there was no release of cytochrome c from the membrane and activation of caspases, and no apoptosis was observed.

5.8 Apoptosis assessment in lung A549 cells treated with the ethyl acetate root extract

Apoptosis is the programmed cell death mechanism used by cells to maintain homeostasis between cell death and cell proliferation. However, the cancerous cells have an uncontrollable proliferation higher than apoptosis. In drug discovery, an ideal drug must have the potential to induce apoptosis by targeting only the cancerous cells, with little or no harm to normal cells. Apoptosis is characterised by different factors which include membrane blebbing, cell shrinkage, chromatin condensation and DNA fragmentation (Behzad *et al*., 2016). Dual staining with acridine orange and ethidium bromide (AO/EB) allows for simultaneous identification of viable and compromised cells.

The orange colour is an indicator of apoptotic features while the green colour is an indicator of viable cells with an intact mitochondrion. The results in Figure 4.12 show that 200 µg/ml SIR-EA extract induced apoptosis following 24 hrs of treatment and nuclear fragmentation was observed, as indicated by an orange staining of the nucleus. The results were the same as the findings by Behzad *et al*. (2016) where it was shown that cells at early apoptosis depict a fragmented nuclear, and the cells undergoing late apoptosis stained yellow-orange because they've lost their membrane integrity and undergone condensation. The apoptosis profile is used to quantify the level of apoptosis at each stage and the results in Figure 4.13 depict that treatment with 200 µg/ml SIR-EA at a percentage of 13.46% did not induce early apoptosis compared to curcumin (28.19%). On the other hand, a significant accumulation of cells in the late apoptosis phase was observed following treatment with 200 µg/ml of SIR-EA (8.85%) as compared to the treatment with curcumin (4.56%).

5.8.2 Microarray analysis

The results in Figure 4.14 depict that, after treatment with SIR-EA extract, the extrinsic pathway is activated by the tumour necrosis factor (TNF). The activation is mediated by the signal through the death receptors bound to the membrane and these death receptors belong to the tumour necrosis factor (TNF) gene superfamily. The interaction of the tumour necrosis factor and tumour necrosis factor receptor (TNFR) lead to the activation of other TNF superfamily members, such as CDL40LG, which is also known as TNFSF5. CDL40LG, through the interaction of TNF and TNFR, leads to the binding and activation of TRADD, which is known to activate pro-caspase-8. The activated pro-caspase-8 leads to an activation of Bid and the intrinsic pathway becomes involved. However, in this study, tBid was downregulated, which is known to activate Bax and Bak in the outer membrane of the cell, leading to the release of cytochrome c activating the intrinsic pathway. The results further suggest that the mitochondria are still intact with no leakage of the mitochondrial contents into the cytosol. The Bcl-2 family (pro-apoptotic) of proteins also triggers the permeabilization of the cell membrane. Bcl-2 family members (anti-apoptotic) function to protect and ensure that the integrity of the membrane of the mitochondria is not compromised (Kiraz *et al*., 2016). The results further prove that after the upregulation of BCL2L11 (pro-apoptotic gene), the mitochondrion are still intact showing that no cytochrome c was released into the cytosol, which is known to form part of the apoptosome. The apoptosome is a complex leading to apoptosis and it was not formed due to the down- regulation of SMAC/DIABLO, which is known to inhibit the effect of the anti-apoptotic gene (XIAP) leading to the compromised mitochondria. However, due to the high up- regulation of XIAP, there was inhibition in the release of cytochrome c from the mitochondria. Amongst all the IAPs, XIAP is the most common inhibitor of apoptosis, making it the centre control of apoptosis through its inhibition of the caspases. The overall results show that despite the activated extrinsic pathway, the cells did not undergo apoptosis, suggesting that the insult to cells by SIR-EA was not potent enough to sustain the state of apoptosis in lung cancer cells.

6. CONCLUSION

The SIR-EA, SIR-Met, SIL-EA and SIL-Met extracts have been shown to have different types of phytochemicals with different compositions of antioxidants. Amongst the four plant extracts of *Senna italica,* the SIR-EA extract had a cytotoxic effect in the lung A549 cancer cells. The SIR-EA extract reduced viability and proliferation of the lung A549 in a concentration-dependent manner compared to the SIL-EA, SIR-Met and SIL-Met extracts. The SIR-EA extract further induced DNA damage in A549 cells, however the damage was minimal and repairable. The SIR-EA extract induced minimal and repairable DNA damage that negatively affected the potential of the cells to sustain the apoptotic state by down-regulating key pro-apoptotic genes and up-regulating anti-apoptotic genes. Overall, the ethyl acetate root extract displayed a promising anti-cancer therapeutic potential that warrants further investigation to elucidate the identity of the inherent chemical components that are responsible for the observed biological activity.

.

7. REFERENCES

Akula, U.S. and Odhav, B., 2013. In vitro 5-lipoxygenase inhibition of polyphenolic antioxidants from undomesticated plants of South Africa. Journal of Medicinal Plants Research, 2(9), pp.207-212.

Alexander, M., Kim, S.Y. and Cheng, H., 2020. Update 2020: Management of Non-Small Cell Lung Cancer. Lung, pp.1-11.

Alzeer, J., Vummidi, B.R., Arafeh, R., Rimawi, W., Saleem, H. and Luedtke, N.W., 2014. The influence of extraction solvents on the anticancer activities of Palestinian medicinal plants. Journal of Medicinal Plant Research, 8(9), pp.408- 415.

Anand, P., Sundaram, C., Jhurani, S., Kunnumakkara, A.B. and Aggarwal, B.B., 2008. Curcumin and cancer: an “old-age” disease with an “age-old” solution. Cancer Letters, 267(1), pp.133-164.

Ashe, P.C. and Berry, M.D., 2003. Apoptotic signaling cascades. Progress in Neuro-Psychopharmacology and Biological Psychiatry, 27(2), pp.199-214.

Ashkenazi, A., Fairbrother, W.J., Leverson, J.D. and Souers, A.J., 2017. From basic apoptosis discoveries to advanced selective BCL-2 family inhibitors. Nature Reviews Drug Discovery, 16(4), pp.273-284.

Aung, T.N., Qu, Z., Kortschak, R.D. and Adelson, D.L., 2017. Understanding the effectiveness of natural compound mixtures in cancer through their molecular mode of action. International Journal of Molecular Sciences, 18(3), pp.656.

Behzad, S., Ebrahim, K., Mosaddegh, M., Haeri, A., 2016. Primula auriculata extracts exert cytotoxic and apoptotic effects against HT-29 human colon Adenocarcinoma cells. Iran. J. Pharm. Res. 15, pp.311–322.

Bele, A.A. and Khale, A., 2011. An overview on thin layer chromatography. International Journal of Pharmaceutical Sciences and Research, 2(2), p.256.

Benzie, I.F. and Strain, J.J., 1996. The ferric reducing ability of plasma (FRAP) as a measure of “antioxidant power”: the FRAP assay. Analytical Biochemistry, 239(1), pp.70-76.

Bernhoft, A., Flaten, T.P., Holmsen, E., Langmark, F., Norum, K.R., Bal, B.S., Singh, R., Steinnes, E., Aaseth, J.O., 2008. Bioactive compounds in plants-benefits and risks for man and animals. The Norwegian Academy of Science and Letters.

Bradley, S.H., Kennedy, M.P. and Neal, R.D., 2019. Recognising lung cancer in primary care. Advances in Therapy, 36(1), pp.19-30.

Brainard, J. and Farver, C., 2019. The diagnosis of non-small cell lung cancer in the molecular era. Modern Pathology, 32(1), pp.16-26.

Chaabane, W., User, S.D., El-Gazzah, M., Jaksik, R., Sajjadi, E., Rzeszowska-Wolny, J. and Łos, M.J., 2013. Autophagy, apoptosis, mitoptosis and necrosis: interdependence between those pathways and effects on cancer. Archivum Immunologiae et Therapiae Experimentalis, 61(1), pp.43-58.

Chang, C.C., Yang, M.H., Wen, H.M. and Chern, J.C., 2002. Estimation of total flavonoid content in propolis by two complementary colorimetric methods. Journal of Food and Drug Analysis, 10(3).

Chen, G., Wan, X., Yang, G. and Zou, X., 2015. Traffic-related air pollution and lung cancer: A meta-analysis. Thoracic Cancer, 6(3), pp.307-318.

Cole, S.P.C., 1986. Rapid chemosensitivity testing of human lung tumor cells using the MTT assay. Cancer Chemother. Pharmacol. 17, 259–263.

Dabai, Y.U., Kawo, A.H. and Aliyu, R.M., 2012. Phytochemical screening and antibacterial activity of the leaf and root extracts of *Senna italica*. African Journal of Pharmacy and Pharmacology, 6(12), pp.914-918.

de Albuquerque Melo, G.M., Silva, M.C.R., Guimaraes, T.P., Pinheiro, K.M., da Matta, C.B.B., de Queiroz, A.C., Pivatto, M., da Silva Bolzani, V., Alexandre-Moreira, M.S. and Viegas Jr, C., 2014. Leishmanicidal activity of the crude extract, fractions and major piperidine alkaloids from the flowers of *Senna spectabilis*. Phytomedicine, 21(3), pp.277-281.

Denisenko, T.V., Budkevich, I.N. and Zhivotovsky, B., 2018. Cell death-based treatment of lung adenocarcinoma. Cell Death & Disease, 9(2), pp.1-14.

Dilruba, S. and Kalayda, G.V., 2016. Platinum-based drugs: past, present and future.

Cancer Chemotherapy and Pharmacology, 77(6), pp.1103-1124.

Drahansky, M., Paridah, M., Moradbak, A., Mohamed, A., Owolabi, F. and Asniza, M., 2016. We are IntechOpen, the world's leading publisher of Open Access Books Built by scientists, for scientists TOP 1%. Intech, 1(tourism), p.13.

Duistermaat, J.J., Kolk, J.A.C., 2000. Proper Actions. In: Afr J Tradit Complement Altern Med. pp. 93–130.

Dzulkifli, F.A., Mashor, M.Y. and Jaafar, H., 2019. An overview of recent counting methods for Ki67 IHC staining. Journal of Biomedical and Clinical Sciences (JBCS), 3(2), pp.10-17.

El Jemli, M., Kamal, R., Marmouzi, I., Zerrouki, A., Cherrah, Y., Alaoui, K., 2016. Radical-Scavenging activity and ferric reducing ability of *Juniperus thurifera* (L.), *J. oxycedrus* (L.), *J. phoenicea* (L.) and *Tetraclinis articulata* (L.). Adv. Pharmacol. Sci. 2016.

Eloff, J.N., 1998. Which extractant should be used for the screening and isolation of antimicrobial components from plants? Journal of Ethnopharmacology, 60(1), pp.1-8.

Franceschi, S. and Bidoli, E., 1999. The epidemiology of lung cancer. Annals of Oncology, 10, pp.S3-S6.

Gazdar, A.F., Bunn, P.A. and Minna, J.D., 2017. Small-cell lung cancer: what we know, what we need to know and the path forward. Nature Reviews Cancer, 17(12), pp.725-737.

Ghosh, D., 2015. Tannins from foods to combat diseases. Int J Pharm Res Rev, 4(5), pp.40-44.

Goldar, S., Khaniani, M.S., Derakhshan, S.M. and Baradaran, B., 2015. Molecular mechanisms of apoptosis and roles in cancer development and treatment. Asian Pacific Journal of Cancer Prevention, 16(6), pp.2129-2144.

Gomes, M., Teixeira, A.L., Coelho, A., Araújo, A., Medeiros, R., 2017. Inflammation and lung cancer: Oxidative stress, ROS, and DNA damage. React. Oxyg. Species Biol. Hum. Heal. Pp.215–223.

Guan, X., 2015. Cancer metastases: challenges and opportunities. Acta Pharmaceutica Sinica B, 5(5), pp.402-418.

Hassanpour, S., Maheri-Sis, N., Eshratkhah, B., & Mehmandar, F.B., 2011. Plants and secondary metabolites (Tannins): A Review. International Journal of Forest, Soil and Erosion (IJFSE), 1(1), 47-53. Int. J. For. Soil Eros. 1, pp.47–53.

Hecht, S.S., 2012. Lung carcinogenesis by tobacco smoke. International Journal of Cancer, 131(12), pp.2724-2732.

Jothi, R.S., Bharathy, V. and Uthayakumari, F., 2015. Antioxidant potential of aerial part of *Senna italica* sub species *micrantha* Mill. Journal of Pharmaceutical Sciences and Research, 7(9), p.621.

Kalemkerian, G.P., 2016, October. Small cell lung cancer. In Seminars in respiratory and critical care medicine (Vol. 37, No. 05, pp. 783-796). Thieme Medical Publishers.

Khalaf, O.M., Ghareeb, M.A., Saad, A.M., Madkour, H.M., El-Ziaty, A.K. and Abdel-Aziz, M.S., 2019. Phenolic constituents, antimicrobial, antioxidant, and anticancer activities of ethyl acetate and n-butanol extracts of *Senna italica*. Acta Chromatographica, 31(2), pp.138-145.

Kim, A., Ko, H.J., Kwon, J.H. and Lee, J.M., 2018. Exposure to secondhand smoke and risk of cancer in never smokers: a meta-analysis of epidemiologic studies. International Journal of Environmental Research and Public Health, 15(9), p.1981.

Kiraz, Y., Adan, A., Yandim, M.K. and Baran, Y., 2016. Major apoptotic mechanisms and genes involved in apoptosis. Tumor Biology, 37(7), pp.8471-8486.

Koegelenberg, C.F.N., Van der Made, T., Taljaard, J.J. and Irusen, E.M., 2016. The impact of HIV infection on the presentation of lung cancer in South Africa. South African Medical Journal, 106(7), pp.666-668.

Kotze, M., Eloff, J.N. and Houghton, P.J., 2002. Extraction of antibacterial compounds from *Combretum microphyllum* (Combretaceae). South African Journal of Botany, 68(1), pp.62-67.

Kurt, O.K., Zhang, J. and Pinkerton, K.E., 2016. Pulmonary health effects of air

pollution. Current Opinion in Pulmonary Medicine, 22(2), p.138.

Labiad, M.H., Harhar, H., Ghanimi, A. and Tabyaoui, M., 2017. Phytochemical screening and antioxidant activity of Moroccan *Thymus satureioïdes* extracts. Journal of Materials and Environmental Sciences, *8*(6), pp.2132-2139.

Leist, M. and Jäättelä, M., 2001. Four deaths and a funeral: from caspases to alternative mechanisms. Nature Reviews Molecular Cell Biology, 2(8), pp.589- 598.

Lemjabbar-Alaoui, H., Hassan, O.U., Yang, Y.W. and Buchanan, P., 2015. Lung cancer: Biology and treatment options. Biochimica et Biophysica Acta (BBA)-Reviews on Cancer, 1856(2), pp.189-210.

Lin, D., Xiao, M., Zhao, J., Li, Z., Xing, B., Li, X., Kong, M., Li, L., Zhang, Q., Liu, Y. and Chen, H., 2016. An overview of plant phenolic compounds and their importance in human nutrition and management of type 2 diabetes. Molecules, 21(10), p.1374.

Loreto, C., La Rocca, G., Anzalone, R., Caltabiano, R., Vespasiani, G., Castorina, S., Ralph, D.J., Cellek, S., Musumeci, G., Giunta, S. and Djinovic, R., 2014. The role of intrinsic pathway in apoptosis activation and progression in Peyronie's disease. BioMed Research International, 2014.

Luo, S. and Rubinsztein, D.C., 2013. BCL2L11/BIM: a novel molecular link between autophagy and apoptosis. Autophagy, 9(1), pp.104-105.

Ly, A., 2018. Traditional Medicines and Cancer Therapies in African Landscape. Journal of Tumor Medicine & Prevention, 3(1), p.555601.

M.H. Labiad, H. Harhar, A. Ghanimi, M.T., 2014. Phytochemical Screening and Antioxidant Activity of Rhizome Extracts. J. Acad. Ind. Res. 3, pp.40–47.

Mahdi-Pour, B., Jothy, S.L., Latha, L.Y., Chen, Y. and Sasidharan, S., 2012. Antioxidant activity of methanol extracts of different parts of *Lantana camara*. Asian Pacific Journal of Tropical Biomedicine, 2(12), pp.960-965.

Maia, I.R.D.O., Trevisan, M.T.S., Silva, M.G.D.V., Breuer, A. and Owen, R.W., 2019. Characterization and Quantitation of Polyphenolic Compounds in *Senna*

macranthera var pudibunda From the Northeast of Brazil. Natural Product Communications, 14(7), p.1934578X19851704.

Masoko, P., Gololo, S.S., Mokgotho, M.P., Eloff, J.N., Howard, R.L., Mampuru, L.J., 2010. Evaluation of the antioxidant, antibacterial, and antiproliferative activities of the acetone extract of the roots of *Senna italica* (Fabaceae). African J. Tradit. Complement. Altern. Med. 7, pp.138–148.

Maxwell, S.A. and Davis, G.E., 2000. Differential gene expression in p53-mediated apoptosis-resistant vs. apoptosis-sensitive tumor cell lines. Proceedings of the National Academy of Sciences, 97(24), pp.13009-13014.

Meerloo, J. Van, Kaspers, G.J.L., Cloos, J., 2011. Cancer Cell Culture: Cell sensitivity assays: The MTT assay 731, 237–245.

Milovanovic, I.S., Stjepanovic, M. and Mitrovic, D., 2017. Distribution patterns of the metastases of the lung carcinoma in relation to histological type of the primary tumor: An autopsy study. Annals of Thoracic Medicine, 12(3), p.191.

Miret, S., De Groene, E.M. and Klaffke, W., 2006. Comparison of in vitro assays of cellular toxicity in the human hepatic cell line HepG2. Journal of Biomolecular Screening, 11(2), pp.184-193.

Mokgotho, M.P., Gololo, S.S., Masoko, P., Mdee, L.K., Mbazima, V., Shai, L.J., Bagla, V.P., Eloff, J.N., Mampuru, L., 2013. Isolation and chemical structural characterisation of a compound with antioxidant activity from the roots of *Senna italica*. Evidence-based Complement. Altern. Med. 2013.

Mustafa, M., Azizi, J., Azizan, N., Jamalulazizi, A.R., Nazirah, A., Abbas, S.A., 2016a. Lung Cancer: Risk Factors, Management, And Prognosis. J. Dent. Med. Sci. 15, pp.94–101.

Mustafa, M., Jamalulazizi, A.R., Iiizam, E.L., Nazirah, A., Abbas, S.A., 2016b. Lung Cancer : Risk Factors, Management , And Prognosis Lung Cancer : Risk Factors , Management , And Prognosis.

Oyebode, O., Kandala, N.B., Chilton, P.J. and Lilford, R.J., 2016. Use of traditional medicine in middle-income countries: a WHO-SAGE study. Health Policy and Planning, 31(8), pp.984-991.

O'Keeffe, L.M., Taylor, G., Huxley, R.R., Mitchell, P., Woodward, M. and Peters, S.A., 2018. Smoking as a risk factor for lung cancer in women and men: a

systematic review and meta-analysis. BMJ Open, 8(10), p.e021611.

Palai, T.K. and Mishra, S.R., 2015. Caspases: An apoptosis mediator. Journal of Advanced Veterinary and Animal Research, 2(1), pp.18-22.

Pascaline, J., Charles, M., Lukhoba, C. and George, O., 2011. Phytochemical constituents of some medicinal plants used by the Nandis of South Nandi District, Kenya. Journal of Animal & Plant Sciences, 9(3), pp.1201-1210.

Patel, S.S. and Savjani, J.K., 2015. Systematic review of plant steroids as potential antiinflammatory agents: Current status and future perspectives. The Journal of Phytopharmacology, 4(2), pp.121-125.

Pfeffer, C.M. and Singh, A.T., 2018. Apoptosis: a target for anticancer therapy. International Journal of Molecular Sciences, 19(2), p.448.

Piluzza, G. and Bullitta, S., 2011. Correlations between phenolic content and antioxidant properties in twenty-four plant species of traditional ethnoveterinary use in the Mediterranean area. Pharmaceutical Biology, 49(3), pp.240-247.

Prasad, S., Gupta, S.C. and Tyagi, A.K., 2017. Reactive oxygen species (ROS) and cancer: Role of antioxidative nutraceuticals. Cancer Letters, 387, pp.95-105.

Priya, M.L., Priya, K.B., Kotakadi, V.S. and Josthna, P., 2015. Herbal and medicinal plants molecules towards treatment of cancer: A mini review. Am J Ethnomed, 2, pp.136-42.

Romagnolo, D.F. and Selmin, O.I., 2012. Flavonoids and cancer prevention: a review of the evidence. Journal of Nutrition in Gerontology and Geriatrics, 31(3), pp.206-238.

Ropiak, H.M., Ramsay, A. and Mueller-Harvey, I., 2016. Condensed tannins in extracts from European medicinal plants and herbal products. Journal of Pharmaceutical and Biomedical Analysis, 121, pp.225-231.

Roy, P., Mandal, P., Panda, S., Roy, S.M. and Subba, A., 2018. Pharmacognosy and phytochemical screening of some plant derived medicine to treat dysmenorrheal pain by the Rajbanshi Community. Pharmacognosy Journal, 10(4).

Sawadogo, W.R., Schumacher, M., Teiten, M.H., Dicato, M. and Diederich, M., 2012.

Traditional West African pharmacopeia, plants and derived compounds for cancer therapy. Biochemical Pharmacology, 84(10), pp.1225-1240.

Sermakkani, M. and Thangapandian, V., 2012. GC-MS analysis of *Cassia italica* leaf methanol extract. Asian J Pharm Clin Res, 5(2), pp.90-94.

Shah, P. and Modi, H.A., 2015. Comparative study of DPPH, ABTS and FRAP assays for determination of antioxidant activity. Int J Res Appl Sci Eng Technol, 3(6), pp.636-41.

Shankar, A., Saini, D., Dubey, A., Roy, S., Bharati, S.J., Singh, N., Khanna, M., Prasad, C.P., Singh, M., Kumar, S., Sirohi, B., Seth, T., Rinki, M., Mohan, A., Guleria, R., Rath, G.K., 2019. Feasibility of lung cancer screening in developing countries: challenges, opportunities and way forward. Transl. Lung Cancer Res. 8, S106–S121.

Sheel, R., Nisha, K. and Kumar, J., 2014. Preliminary phytochemical screening of methanolic extract of *Clerodendron infortunatum*. IOSR Journal of Applied Chemistry, 7(1), pp.10-13.

Shishir, T.A., Khan, R.I. and Nirzhor, S.S.R., 2018. The critical role of tumor microenvironment in cancer evolution and metastasis. International Journal of Business Research, 9(7), pp.244-258.

Shunmuga Jothi, R., Bharathy, V., Uthayakumari, F., 2015. Antioxidant potential of aerial part of *Senna italica* sub species *micrantha* Mill. J. Pharm. Sci. Res. 7, 621–625.

Singh, S., Sharma, B., Kanwar, S.S. and Kumar, A., 2016. Lead phytochemicals for anticancer drug development. Frontiers in Plant Science, 7, p.1667.

Srivastava, S., Somasagara, R.R., Hegde, M., Nishana, M., Tadi, S.K., Srivastava, M., Choudhary, B. and Raghavan, S.C., 2016. Quercetin, a natural flavonoid interacts with DNA, arrests cell cycle and causes tumor regression by activating mitochondrial pathway of apoptosis. Scientific Reports, 6, p.24049.

Steenkamp, V. and Gouws, M.C., 2006. Cytotoxicity of six South African medicinal plant extracts used in the treatment of cancer. South African Journal of Botany, 72(4), pp.630-633.

Sudhakar, A., 2009. History of cancer, ancient and modern treatment methods. Journal of Cancer Science & Therapy, 1(2), p.1.

Sultan, A. and Raza, A.R., 2015. Steroids: A diverse class of secondary metabolites. Med Chem, 5(7), pp.310-317.

Swift, L.H. and Golsteyn, R.M., 2014. Genotoxic anti-cancer agents and their relationship to DNA damage, mitosis, and checkpoint adaptation in proliferating cancer cells. International Journal of Molecular Sciences, 15(3), pp.3403-3431.

Syed Abdul Rahman, S.N., Abdul Wahab, N., Abd Malek, S.N., 2013. *In Vitro* Morphological Assessment of Apoptosis Induced by Antiproliferative Constituents from the Rhizomes of *Curcuma zedoaria*. Evidence-Based Complement. Altern. Med. 2013, 1–14.

Taylor, J.L.S., Rabe, T., McGaw, L.J., Jäger, A.K. and Van Staden, J., 2001. Towards the scientific validation of traditional medicinal plants. Plant Growth Regulation, 34(1), pp.23-37.

Thoppil, R.J. and Bishayee, A., 2011. Terpenoids as potential chemopreventive and therapeutic agents in liver cancer. World Journal of Hepatology, 3(9), p.228.

Vaghasiya, Y., Dave, R., Chanda, S., 2011. Phytochemical analysis of some medicinal plants from western region of India. Res. J. Med. Plant 5, 567–576.

Wang, J.J., Lei, K.F. and Han, F., 2018. Tumor microenvironment: recent advances in various cancer treatments. Eur. Rev. Med. Pharmacol. Sci, 22, pp.3855-3864.

Wang, T.Y., Li, Q. and Bi, K.S., 2018. Bioactive flavonoids in medicinal plants: Structure, activity and biological fate. Asian Journal of Pharmaceutical Sciences, 13(1), pp.12-23.

Wang, X. and Guo, Z., 2013. Targeting and delivery of platinum-based anticancer drugs. Chemical Society Reviews, 42(1), pp.202-224.

Widyawati, P.S., Budianta, T.D.W., Kusuma, F.A. and Wijaya, E.L., 2014. Difference of solvent polarity to phytochemical content and antioxidant activity of Pluchea indicia less leaves extracts. International Journal of Pharmacognosy and Phytochemical Research, 6(4), pp.850-855.

Wong, R.S., 2011. Apoptosis in cancer: from pathogenesis to treatment. Journal of Experimental & Clinical Cancer Research, 30(1), p.87.

Yuan, H., Ma, Q., Ye, L. and Piao, G., 2016. The traditional medicine and modern medicine from natural products. Molecules, 21(5), p.559.

Zappa, C. and Mousa, S.A., 2016. Non-small cell lung cancer: current treatment and future advances. Translational Lung Cancer Research, 5(3), p.288.

Zhang, Y., Chen, X., Gueydan, C. and Han, J., 2018. Plasma membrane changes during programmed cell deaths. Cell Research, 28(1), pp.9-21.

Zheng, M., 2016. Classification and pathology of lung cancer. Surgical Oncology Clinics, 25(3), pp.447-468.